F I E L D G U I D E

CETEG 2015

13th Meeting of the Central European Tectonic Groups

Early Variscan (and pre-Variscan) evolution of the western part of the Teplá-Barrandian Unit

Vít Peřestý, Ondrej Lexa, Petr Jeřábek, Martin Racek

14 millions years of the volcanic history of Doupovské hory Volcanic Complex

Vladislav Rapprich and Michael Petronis

The meeting is organized by
Czech Geological Survey
Faculty of Science, Charles University in Prague

Organizing team
Pavlína Hasalová, Ondrej Lexa & Petr Jeřábek

Central European Tectonic Groups Annual Meeting – CETEG 2015

Edited by Ondrej Lexa, Vít Peřestý, Petr Jeřábek, Pavlína Hasalová,
Martin Racek, Vladislav Rapprich & Michael Petronis

Printed & published by the Czech Geological Survey
Klárov 3, 118 21 Prague 1, Czech Republic
First edition, 42 pages, 85 copies
03/9 446-406-15
ISBN 978-80-7075-881-6

Early Variscan (and pre-Variscan) evolution of the western part of the Teplá-Barrandian Unit

Vít Peřestý, Ondrej Lexa, Petr Jeřábek, Martin Racek

The Bohemian Massif is located at the eastern extremity of the European Variscan belt representing one of its largest exposures (Fig. 1). From west to the east, the Eastern Variscan belt forming the Bohemian Massif can be subdivided into four major units: 1) The Saxothuringian Neoproterozoic basement with its Palaeozoic cover corresponding to continental crust of the Armorican plate (Franke, 2000); 2) The Teplá-Barrandian Unit consisting of Neoproterozoic basement and its Early Palaeozoic cover interpreted as an independent crustal block (the Bohemia Terrane of South Armorica sensu Tait et al. (1997); 3) The Moldanubian high- to medium-grade metamorphic domain intruded by numerous Carboniferous granitic plutons, altogether forming the high-grade core of the orogen; and 4) The easterly Brunia Neo-Proterozoic basement with Early to Late Palaeozoic cover (Dudek, 1980; Finger et al., 2000; Kalvoda et al., 2008).

The aim of the pre-conference field trip is to present the state-of-art data and interpretations related to structural and metamorphic evolution of the western part of the Bohemian Massif with special focus on the Teplá–Barrandian Unit. The main objective is to discuss deformation history recorded in the orogenic supra-structure and relate it to the processes operating simultaneously in the orogenic infra-structure. Following paragraphs provide a reader with overall description of key domains in the region (Fig. 2).

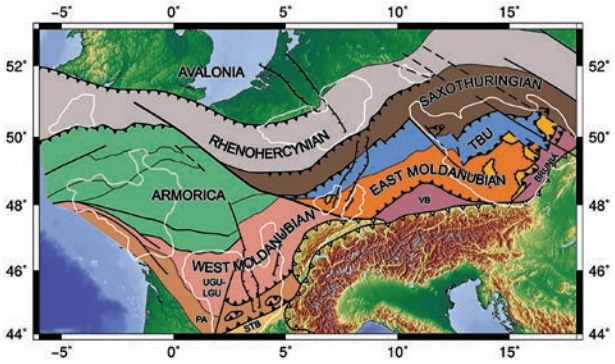

Fig. 1: Schematic figure of European Variscan belt.

Saxothuringian domain

This domain is represented by Neoproterozoic par-autochthonous rocks (580–550 Ma) formed by migmatites and paragneisses intruded by Cambro–Ordovician calc-alkaline porphyritic granitoids converted to augen orthogneiss during the Variscan orogeny (Košler et al., 2004; Kröner et al., 1995; Siebel et al., 1997; Tichomirowa et al., 2001). These rocks are unconformably covered by Cambrian and Ordovician rift sequences overlain by Late Ordovician to Famennian pelagic sediments and Famennian to Visean flysch of the Thuringian facies (Franke, 2000). The par-autochthon is overthrusted by allochthonous units containing deep water equivalents of the Ordovician to Devonian rocks of the par-autochthon, and by proximal flysch sediments (the Bavarian facies). The allochthonous units occur in Münchberg, Wildenfels and Frankenberg klippens and exhibit pile of thrust sheets marked by decreasing pressure and age of metamorphism from eclogitized metabasites of Ordovician protolith age (Stosch and Lugmair, 1990; O'Brien and Carswell, 1993) in hangingwall to rocks marked by medium-pressure assemblages and Late Devonian (~365 Ma) zircon and hornblende cooling ages in the footwall. This rock pile is interpreted to represent both distal and proximal Late Ordovician to Devonian passive margin rocks tectonically inverted during the Devonian convergence (Franke, 2000). However, the underthrusting of the Saxothuringian/Armorican continental rocks underneath the easterly Teplá-Barrandian block suggests a continuous convergence in this area, which was responsible for eclogitization of both the oceanic and continental crust (Konopásek and Schulmann, 2005). The continental underthrusting reached pressure conditions in the stability field of diamond (Massonne, 2006; Kotková et al., 2011).

The Saxothuringian and Teplá–Barrandian boundary

The boundary between the two crustal domains is characterized by the presence of units with high proportion of ultramafic and mafic rocks; the Mariánské Lázně Complex and Erbendorf–Vohenstrauss Zone. The former complex is marked by a presence of serpentinites

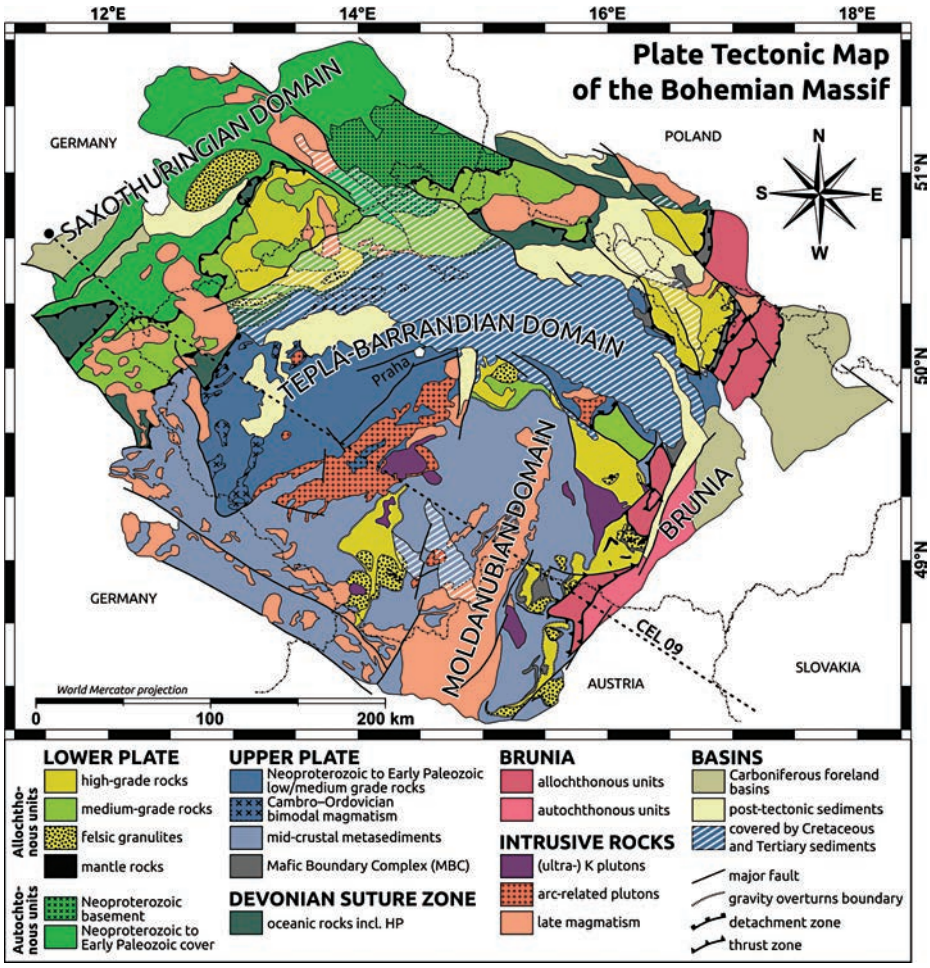

Fig. 2: Tectonic map of the Bohemian Massif from Schulmann et al. (2014).

at its structural bottom overlain by amphibolites with lenses of eclogite, rarely with coronitic metagabbro, and intercalations of paragneiss and orthogneiss (e.g., Jelínek et al., 1997; Štědrá, 2001; Fiala, 1958). Several metagabbro bodies (up to 2 × 10 km in size) with relict igneous textures are exposed along the southeastern border of the Mariánské Lázně Complex (Štědrá et al., 2002), although some metagabbro also occur adjacent or within the orthogneiss and paragneiss of the Teplá–Barrandian unit (Kachlík, 1997). The U/Pb zircon protolith ages discriminate the mafic rocks into two main groups with Cambrian (~540 Ma; Timmermann et al., 2004) and Ordovician ages (~496 Ma; Bowes and Aftalion, 1991). On the other hand, the metamorphic and cooling ages (Sm-Nd garnet–pyroxene and Ar/Ar hornblende) are Devonian, ranging between 410 and 370 Ma (Beard et al., 1995; Dallmeyer and Urban, 1998). Similarly, the U/Pb ages for metamorphic zircon in mafic rocks, as well as monazite from orthogneiss, and titanite in leucosome all cluster around 380 Ma (Timmermann et al., 2004) and likely date the granulite-facies re-equilibration superposed on eclogite-facies metamorphism (640–715°C at 16–18 kbar; O'Brien, 1997). The Erbendorf–Vohenstrauss Zone further to the west shows similar lithological and petrological zonation as the Mariánské Lázně Complex and it is thus commonly interpreted as a part of the same tectonic unit (Franke, 2000).

Teplá-Barrandian domain

The Teplá-Barrandian Unit (TBU), also known as "Bohemicum" is interpreted as a relic of the Cadomian orogenic belt and consists of Neoproterozoic basement with the lower arc-related volcano-sedimentary sequence (the Kralupy–Zbraslav Group), followed by siliceous black shales and a flyschoid sequence (Kříbek et al., 2000; Drost et al., 2004). The Neoproterozoic basement is unconformably overlain by a thick sequence (1500–2000 m) of Lower Cambrian conglomerates, greywackes, and sandstones (Dörr et al., 2002) followed by shales and a rift-related volcanic sequence in the Upper Cambrian (Pin and Waldhausrová, 2007). The development of the Lower Palaeozoic Prague Basin is marked by Early Ordovician (Tremadocian) transgression followed by mid-Ordovician rifting associated with volcanic activity, and with sedimentation of Silurian graptolite shales. The sedimentation continued mainly

by carbonates, namely the Upper Silurian to Devonian calcareous flyschoid sequence. The Early Silurian was associated with important volcanic activity accompanied by basaltic and ultramafic intrusions (Patočka et al., 1993). The sedimentation terminated in mid-Devonian with distal turbidites of the Srbsko Formation (Givetian) containing, among others, detrital zircons of Devonian age (~390 Ma; Strnad and Mihaljevič, 2005). The western part of the TBU consists of Domažlice and Teplá Crystalline Complexes (DCC and TCC) considered as a metamorphosed equivalents of the lower part of the Kralupy–Zbraslav Group (Vejnar, 1984).

The Proterozoic rocks are intruded by bodies of Cambrian and Devonian granites (Dörr et al., 1998; Venera et al., 2000). Towards the west and northwest the metamorphic grade of the Proterozoic rocks increases up to kyanite facies in the Domažlice and Teplá Crystalline complexes, respectively. The metamorphism in the Domažlice Crystalline Complex is associated with Cadomian event (Zulauf et al., 1997) whereas in the Teplá Crystalline Complex it is associated with the early phases of Variscan orogeny (Žáček and Cháb, 1998; Žáček, 1999; Zulauf, 2001; Timmermann et al., 2006). The Teplá Crystalline Complex is composed mostly of medium grade metasediments (phyllite, metagraywacke and micaschist) with well-developed Barrovian metamorphic zonation (Žáček and Cháb, 1993) and associated small bodies of Late Cambrian granitoids and pegmatites (504–528 Ma and 475–487 Ma respectively; Glodny et al., 1998; Dörr et al., 1998; Venera et al., 2000).

The Cadomian evolution of the Neoproterozoic rocks of the Teplá–Barrandian Unit is comparable with the northern part of the Armorican Massif and comprises: (1) formation of volcanic arc, back-arc basin and remnant arc; (2) basin inversion and probably polyphase orogenic deformation associated with synorogenic sedimentation; and (3) post-Cadomian extension period associated with the formation of Cambrian basins (Kříbek et al., 2000; Hajná et al., 2010, 2011).

Recent view on the Variscan geodynamic evolution of the Bohemian massif

Starting with Suess (1926), the structure of the Bohemian Massif was explained as a result of large-scale tangential tectonics. It was suggested by Matte et al. (1990) that the Variscan orogeny was governed by successive stacking of thrust sheets, while Dewey and Burke (1973) proposed a model of homogeneous thickening and magmatic recycling. Later, Schulmann et al. (2009) interpreted the Bohemian Massif as an Andean type supra-subduction orogen of double crustal thickness developed over the width of at least 500 km in the present coordinates. According to those authors, Variscan Bohemian Massif is a result of an Early Devonian subduction of the Saxothuringian ocean of unknown size underneath the easterly continental plate represented by the present-day Teplá–Barrandian and Moldanubian Domains. During mid-Devonian the Saxothuringian passive margin sequences and relics of Ordovician oceanic crust have been obducted over the Saxothuringian basement in conjunction with an extrusion of the Teplá–Barrandian middle crust along the so-called Teplá suture zone. This event was connected with the development of magmatic arc further east together with a fore-arc basin on the Teplá-Barrandian crust. The back arc region – the future Moldanubian zone – was affected by lithospheric thinning which marginally affected also the easterly continental crust of Brunia. The subduction stage was followed by collisional event caused by the Saxothuringian continental crust entering the subduction domain (Fig. 3). This was associated with crustal thickening and development of the orogenic root system in the magmatic arc and back-arc region of the orogen. The thickening was associated with deepening of Moho and influx of the Saxothuringian felsic crust into the root domain. Originally subhorizontal anisotropy in the root zone was subsequently affected by crustal-scale cusp folds developed in the front of the Brunia back stop. During Viséan the Brunia indented the thickened crustal root resulting in its massive shortening and vertical extrusion of the orogenic lower crust, which evolved into horizontal flow in the mid- to supra-crustal levels (Fig. 3).

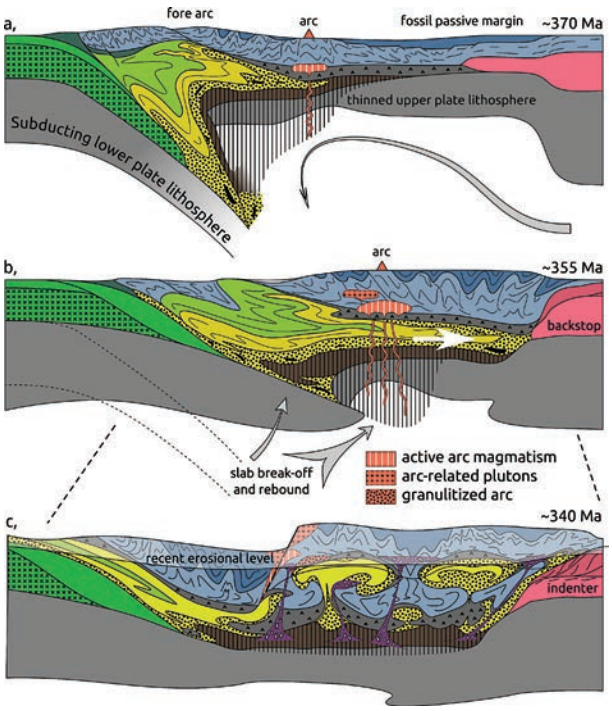

Fig. 3: Model of the Variscan tectonic evolution of the Bohemian Massif after Schulmann et al. (2014).

The current progress in structural geology, petrology, geochemistry and geochronology (Schulmann et al., 2009; Lexa et al., 2011; Schulmann et al., 2014) enabled assignment of individual crustal units of the Bohemian Massif to three distinct precursors (Fig. 2):

- the upper plate represented by orogenic supra-structure (the Teplá–Barrandian domain) and mid-crustal units (Monotonous and Varied groups) incorporated into orogenic root (the Moldanubian domain);
- the lower plate occurring as a coherent Saxothuringian domain in the west and high-grade felsic meta-igneous complexes (HP granulites and orthogneisses of the so-called Gföhl Unit) emerging in the internal part of the Moldanubian domain as two NE–SW trending belts;
- continental back-stop (Brunia) indenting the orogenic root zone from the east

The upper and lower plate boundary is commonly marked by the presence of mafic rocks, including metagabbros, MORB-type eclogites and peridotites (called here the Mafic Boundary Complex – MBC). While, in the west, the MBC forms klippen thrust over weakly metamorphosed rocks of the Saxothuringian domain, further east it disappears under the orogenic supra-structure. In the internal part, however, this important boundary bears a witness to intensity of material exchange between lower and upper plates. It locally led to an inversion of the original rock sequence; a fact once taken as an evidence of the large-scale thrust tectonics (Matte et al., 1990; Tollmann, 1982). For instance, in Lower Austria, the lower-plate-derived high-pressure orthogneisses and felsic granulites, containing relics of MORB-like eclogites, rest upon Late Proterozoic to Early Paleozoic mid-crustal metasediments with orthogneisses of the upper plate. Their boundary is marked by a continuous layer of Early Paleozoic metabasic rocks (MBC).

The geophysical imagery reveals highly reflective crust west of the magmatic arc and blurred seismic fabric to the east (Fig. 4). The western part of the 9HR seismic profile shows east-dipping strong reflector zone in the sub-surface continuity of the MBC. The underlying low-reflectivity and low-velocity zone in the profile CEL-09 is interpreted as a felsic meta-igneous crustal layer of Saxothuringian provenance. Surface projection of this zone coincides with outcrop of felsic orthogneiss to granulite belt located along Saxothuringian – Teplá–Barrandian contact.

Both reflection and refraction seismic studies (Růžek et al., 2003; Tomek et al., 1997) disclose an existence of weakly reflective, low-velocity zone underlying the Moldanubian domain. In addition, the whole 200 km wide domain coincides with a large wavelength gravity low suggesting that the average density of the Moldanubian domain is lower compared to westerly relict of the upper plate and easterly Brunia indentor. The wavelength of negative anomaly is in agreement with the presence of low-velocity layer in the lower crust. While the seismic Moho (discordance in seismic velocities) is approximately flat, the continuation of reflections to the southeast suggests that the seismic does not coincide with petrological Moho. This points to the presence of mafic eclogites, which show seismic properties similar

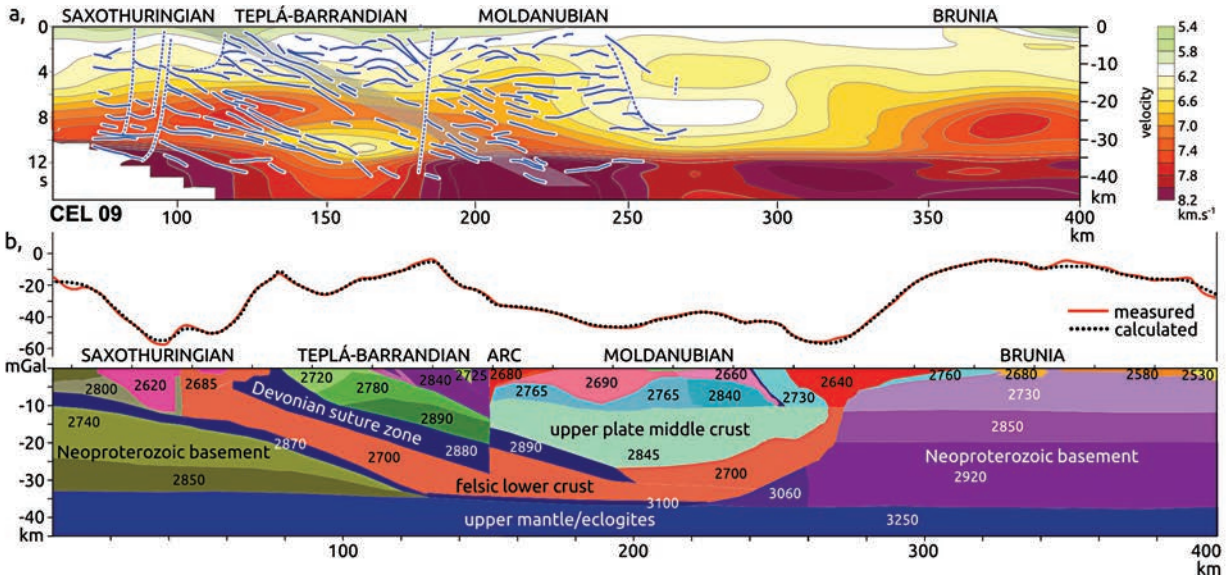

Fig. 4: Geophysical profile across the Bohemian Massif. A: Line drawing of reflection seismic section 9HR superimposed on the seismic refraction section CEL 09. Devonian suture zone is highlighted by gray transparent layer. B: Two-dimensional gravity model showing densities (in kg/m³) attributed to different rock types forming the Bohemian Massif. Curves above depict values of measured (thick dotted) and modeled (solid) Bouguer anomalies. See also Schulmann et al. (2014)

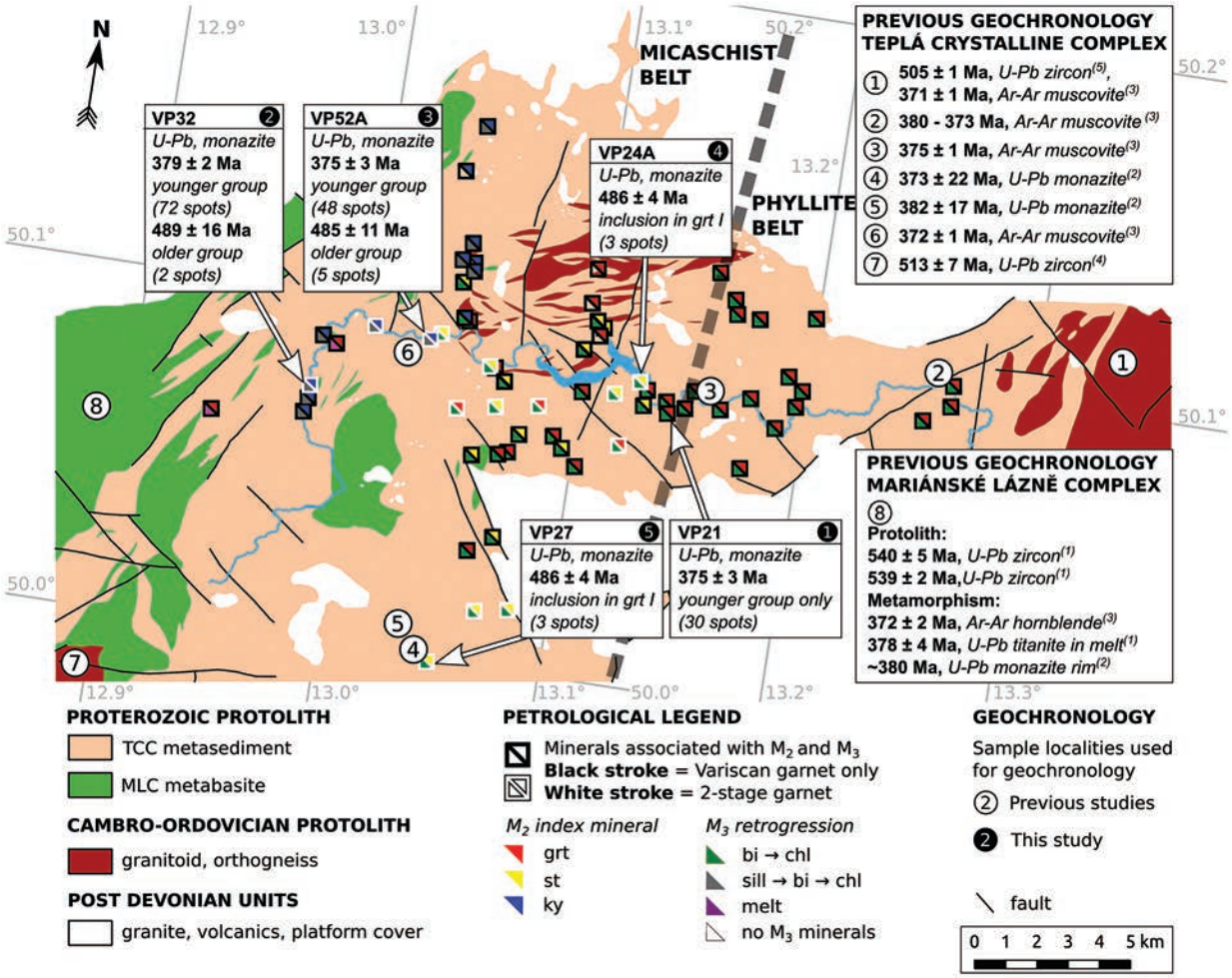

Fig. 5: Simplified geological map of the Teplá Crystalline Complex including both published and new geochronological data together with metamorphic assemblages related to the most prominent metamorphic events M_2 and M_3.

to peridotites (Mengel and Kern, 1992). The eclogites are attributed to the MBC, which is, unlike in the west, located underneath the Saxothuringian felsic material (Fig. 2).

Structural and metamorphic record of the Teplá Crystalline Complex and Mariánské Lázně Complex

TEPLÁ CRYSTALLINE COMPLEX

The TCC shows northwestward Barrovian metamorphic field gradient covering biotite, garnet, staurolite and kyanite zones (Fig. 5) with estimated PT conditions ranging from 450°C at ~3 kbar to 680°C at ~9 kbar (Žáček and Cháb, 1993; Cháb and Žáček, 1994; Žáček and Cháb, 1998; Zulauf, 1997b; Štědrá, 1994). Despite a long-lasting discussion about the age of deformation and metamorphism in the TCC, it is generally accepted that the dominant Barrovian metamorphic field gradient is associated with Variscan orogeny (Žáček and Cháb, 1998; Žáček, 1999; Zulauf, 2001; Timmermann et al., 2006) as documented by solid-state deformation and metamorphism of the Early Paleozoic intrusive rocks (Dörr et al., 1998). The timing of the Variscan metamorphism is constrained by numerous Ar/Ar muscovite and U/Pb monazite ages from the TCC metasediments (385–370 Ma; Fig. 5; Dallmeyer and Urban, 1998; Timmermann et al., 2006). On the other hand, the superposition of deformation structures (Zulauf, 1997b; Žáček and Cháb, 1998; Zulauf, 2001), the common occurrence of two compositional varieties of garnets (Fig. 5. Žáček and Cháb, 1993; Zulauf, 2001) and the pre-Variscan U/Pb monazite ages (ca 540–480 Ma, Timmermann et al., 2006) point to a polyphase evolution of the area.

Only a few studies focusing on deformation structural record in the TCC have been published so far. From these previous studies, the most important appears to be the work of Zulauf (2001) who first described the brittle-ductile transition in mechanical behaviour of the TCC rocks and pointed out the evolution in rheological properties and deformation mechanisms.

Our recent studies in the Teplá Crystalline Complex (TCC) brought large quantity of new structural and metamorphic data and interpretations, which are in

part presented in this guide. Based on our detailed structural analysis, petrographic description and thermodynamic modeling, three distinct deformation (D_1-D_3) and corresponding metamorphic (M_1-M_3) events have been recognized in the studied area. To demonstrate the systematic spatial variations in structural styles and metamorphic conditions associated with individual events, we identified two lithological belts with distinct tectono-metamorphic evolution i.e. the phyllite and micaschist belts (Fig. 5). In general, the phyllite belt

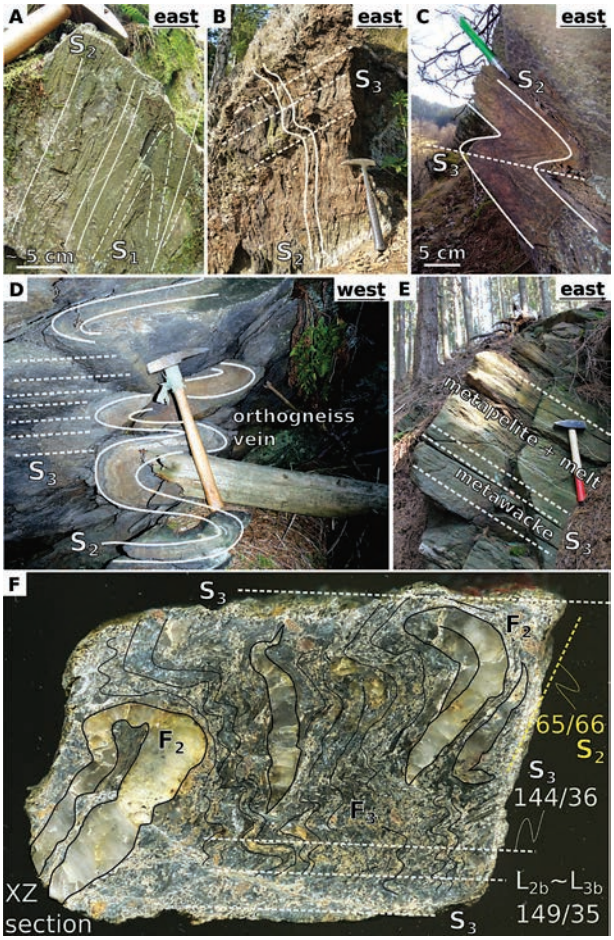

Fig. 6: Structural observations. A) S_1 is folded by F_2 folds with steep axial plane and subhorizontal fold axis. Eastern phyllite belt. B) Penetrative sub-vertical S_2 cleavage is affected by D_3 kink bands with subhorizontal axial plane. Garnet zone in the western phyllite belt. C) Asymmetrical F_3 fold with top-to-the-SE vergence affecting S_2 cleavage. Subhorizontal cleavage parallel to axial plane of F_3 fold is developed only in the less competent layer in the right part of the picture, garnet zone, phyllite/micaschist belt boundary. D) Tight F_3 fold appeared by vein of felsic orthogneiss. Penetrative S_3 cleavage developed in the metasedimentary host is subhorizontal. Micaschist belt, staurolite zone. E) Prolate fabrics in the micaschist belt, kyanite zone. Apparent prolate strain results from high angle superposition of moderately inclined S_3 cleavage onto originally sub-vertical S_2 fabric. S_2 is axial plane of refolded Qtz veins, probably representing trend of S_1 foliation. XZ section.

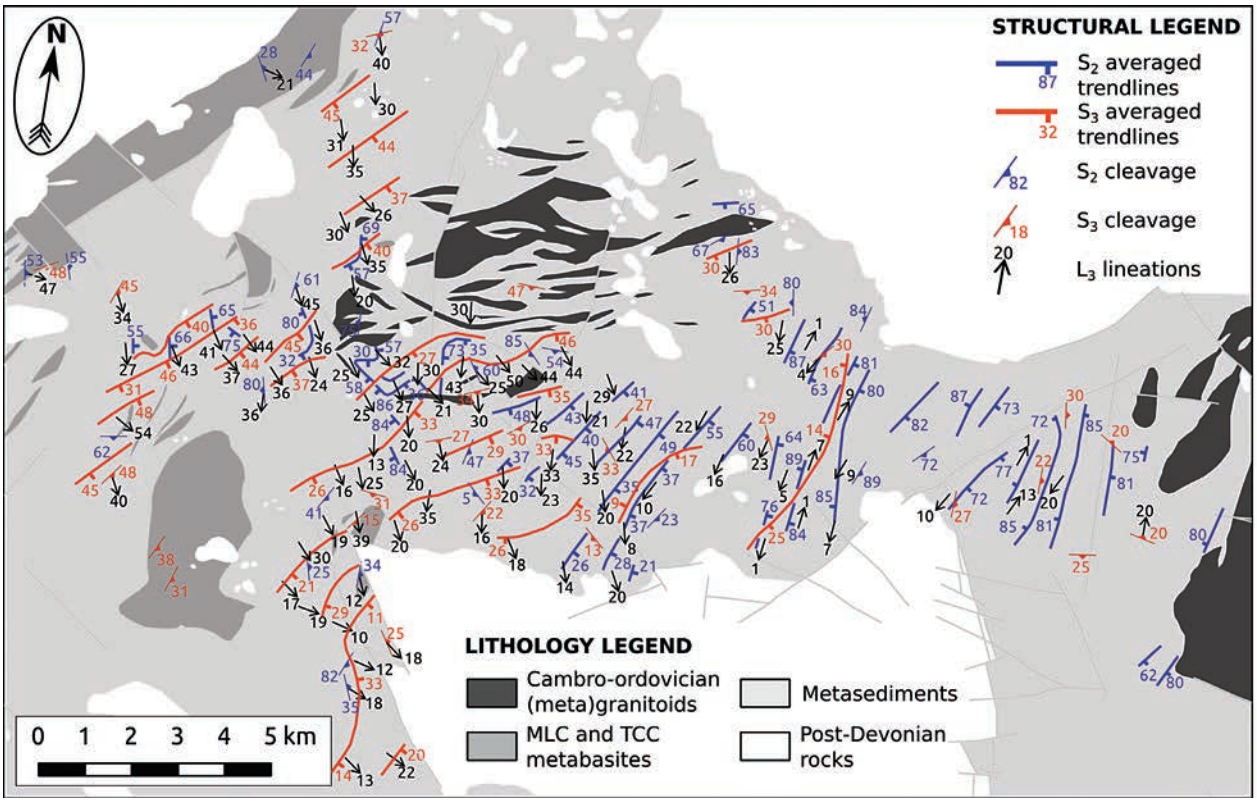

Fig. 7: Structural map of the northern part of the Teplá Crystalline Complex.

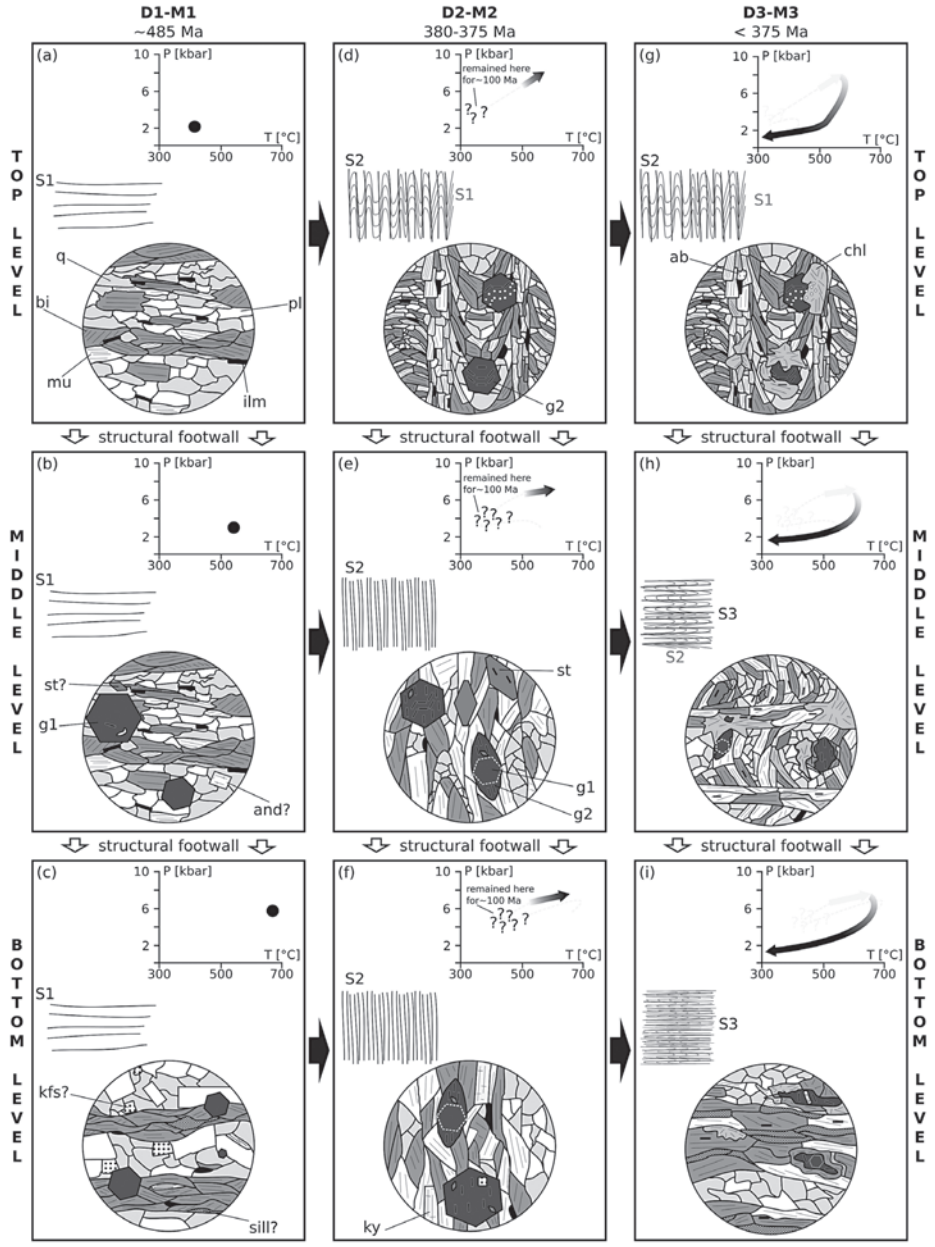

Fig. 8: P-T-D-t evolution scheme for the Teplá Crystalline Complex. For details see text.

preserves the earlier fabrics attributed to D_1 (M_1) and D_2 (M_2), while the micaschist belt is intensely affected by D_3 (M_3) event (Figs. 6 & 7). The following paragraphs characterize the individual deformation events D_1, D_2 and D_3 separately and focus on their deformation styles.

- D_1-M_1 is the first event, where the metamorphic assemblage and deformation fabrics can be directly linked. The original orientation of foliation prior to subsequent deformation is not well constrained, but most likely was sub-horizontal to gently inclined to the south. Lineation associated with this fabric is unknown, but analogous AMS fabrics from Tis granite shows overall oblate symmetry and radial pattern of AMS lineation (Seifert, 2012). D_1 structures are best preserved in the phyllite belt (Fig. 6a).
- D_2 deformation structures dominate the studied area (Fig. 7), also the M_2 metamorphic mineral assemblage is the most prominent in the studied region. The original orientation of S_2 fabric was sub-vertical and N–S trending locally bearing sub-vertical stretching lineation. D_2 structures are best preserved in the phyllite belt (Fig. 6a & b) and become strongly overprinted by D_3 deformation in the micaschist belt towards the west (Figs. 6c-f and 7).
- D_3 deformation is the last event associated with ductile overprint that was recognized in the TCC. The intensity of D_3 increases towards the west and becomes dominant deformation phase within the entire micaschist belt (Fig. 6c-f). D_3 results from sub-vertical shortening and leads to development of subhorizontal to gently SE-dipping cleavage with SSW-plunging lineation in the phyllite belt that rotates to SE- or E-plunging orientation in the micaschist belt (Fig. 7).

Because a near complete upper- to mid-crustal section is exposed in the western part of the TCC, the structural

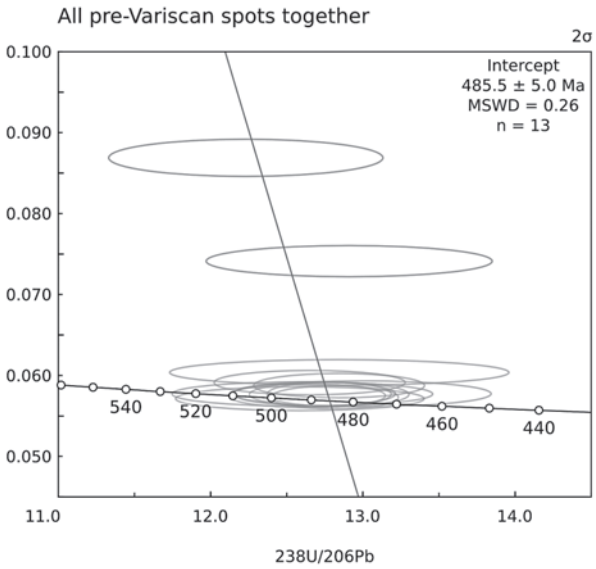

Fig. 9: Monazite LASS ICP-MS U/Pb geochronological data for all observed pre-Variscan ages.

and metamorphic evolution can be demonstrated in a simplified P-T-D-t scheme (Fig. 8). The scheme shows separately the evolution of three crustal levels, i.e. top – corresponding to phyllite belt; middle – corresponding to transition between phyllite and micaschit belts; and bottom – corresponding to micaschist belt.

The first tectono-metamorphic event D_1-M_1 (Fig. 8a-c) is interpreted to be Cambro–Ordovician, based on ~485 Ma U/Pb monazite ages from monazites enclosed in the cores of two-stage garnets (Fig. 9). D_1-M_1 shows normal metamorphic zoning covering biotite (Fig. 8a) and garnet zones (Fig. 8b & c), and possibly also partial melting in the structurally deepest levels, reaching temperatures of at least 650°C at the base of the TCC metasedimentary crust. Composition of garnet (g1) cores suggests overall low-pressure PT path at elevated geothermal gradient around 50°C/km at structurally higher levels (Fig. 8b), which decreases towards deeper parts to 30°C/km (Fig. 8c). Various observations suggest that the original orientation of S_1 was subhorizontal e.g. i) the Tis granite was emplaced as subhorizontal sill (Dobeš et al., 1967) parallel to main anisotropy of host rock at cca 505 Ma (Venera et al., 2000) and ii) L_2 intersection lineation and F_2 fold axes are consistently subhorizontal in upper structural levels.

The subsequent early Variscan D_2-M_2 and D_3-M_3 events (Fig. 10) were temporally very close and represent rather continuous process than two separate tectono-metamorphic events. This is based on i) similar age of Ar/Ar cooling data and U/Pb monazite data (Fig. 5), ii) early-Variscan age of monazite enclosed in the M_2 garnet and iii) statistically the same age of monazite Y-poor cores and Y-rich rims. Y-poor monazite often grow, when the garnet as a major sink for Y was already present. In our case early-Variscan low-Y monazite cores can therefore be attributed to higher temperature part of the prograde M_2 event. Finally M_3 event is characterized by breakdown of garnet, which can be coeval with growth of Y-rich patchy rims (Fig. 10).

The early Variscan convergence is marked by onset of D_2 deformation responsible for development of vertical fabric at all crustal levels (Fig. 11a). D_2-M_2 event is well-documented by transposition and recrystallization of the older fabrics and growth of prograde Barrovian sequence of minerals – garnet (550°C, Fig. 8d), staurolite (600°C, Fig. 8e), kyanite (650°C, Fig. 8f). Garnet (g2) crystallized at every structural level, but g2 is the only garnet generation in the upper level (Fig. 8d), while two-stage garnets are preserved in the deeper levels (Fig. 8e & f).

The prograde part of the early-Variscan PT path is characterized by MP-MT geothermal gradient, which progressively changes from slightly colder geotherm around 20°C/km to normal barrovian geotherm around 25°C/km as the temperature increases. Generally, the colder geotherm (typically ~520°C, 6.5 kbar) is well recorded in the top structural level and diminishes towards structural low by the higher temperature

Fig. 10: Geochronological data from the sample VP32 in the kyanite zone of the micaschist belt. a) U/Pb plot showing both pre-Variscan (red) and early Variscan (grey) analyses, b-e) representative Yttrium compositional maps, f-g) BSE image showing the location of pre-Variscan analyses.

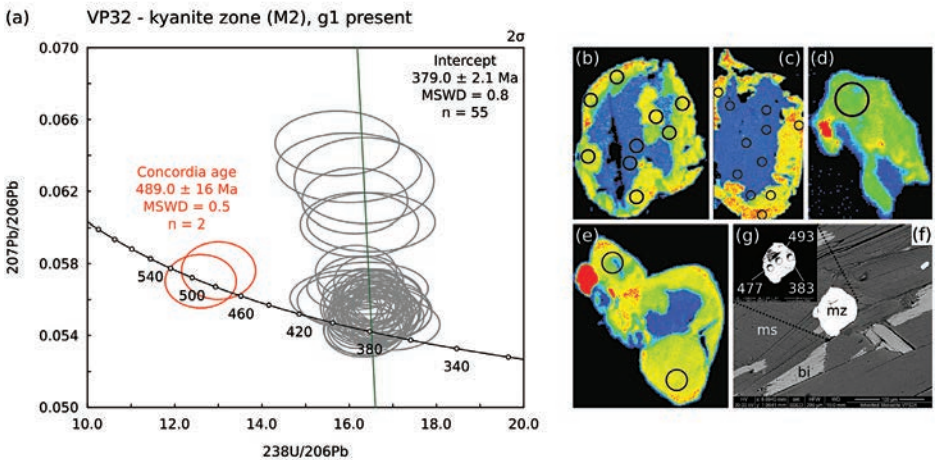

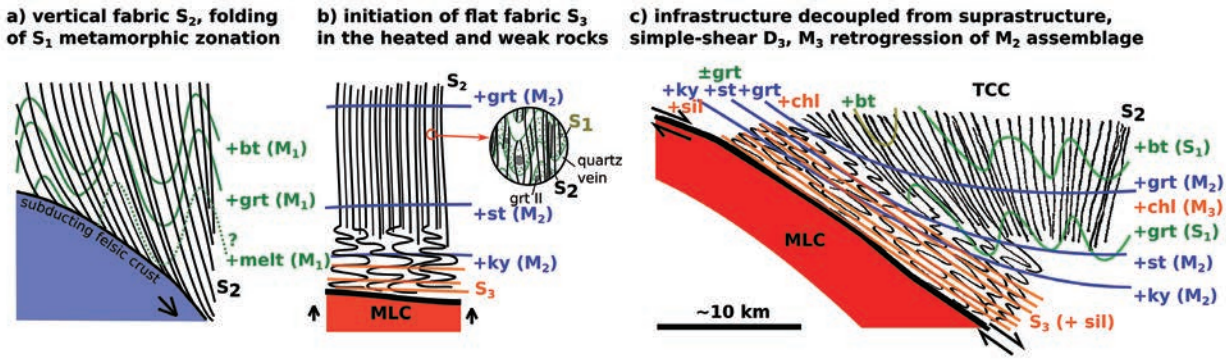

Fig. 11: Early-Variscan tectonic evolution of the Teplá Crystalline Complex. For details see text.

overprint, however still is well documented by the chemistry of g2 cores with paragonite and zoisite inclusions. The temperature peak at the end of prograde PT path corresponds to the transition from D_2-M_2 to D_3-M_3 event (Fig. 11b) and is characterized by temperatures even above wet-solidus line (> 650°C) and partial melting at the deepest structural levels along the contact with MLC. The D_3-M_3 event (Fig. 8g–i) includes both pressure and temperature drop and overall retrogression of peak conditions M_2 mineral assemblage. Despite the M_3 PT condition are not precisely known, the highest M_3 temperatures were reached at the bottom level (Fig. 8i) marked by growth of fibrous sillimanite. As the temperature decreased, garnet was by replaced by biotite and biotite subsequently replaced by chlorite (Fig. 8g-i). In the upper levels the M_3 retrogression is mostly static (Fig. 8g), while in deeper structural levels it is accompanied by deformation D_3 (Fig. 8h & i). D_3 is mostly represented by subhorizontal to gently SE dipping axial planar cleavage that rapidly intensifies towards boundary with MLC.

The most important property of D_3-M_3 event is production of normal metamorphic field zonation (S_3 dips to SE and both M_2 and M_3 show increase in metamorphic grade to NW). D_3-M_3 is interpreted to reflect activity of large-scale detachment responsible for exhumation of deeper levels including pre-Variscan plutonic and LP/HT metamorphic rocks (Fig. 11c).

MARIÁNSKÉ LÁZNĚ COMPLEX

Towards the NW, the peak metamorphism further increases in the structurally lower Mariánské Lázně Complex (MLC) reaching eclogite-facies conditions. The MLC consists of amphibolites, retrogressed eclogites, meta-gabbros and peridotites interpreted as remnant of subducted/exhumed oceanic crust (Kastl and Tonika, 1984; Bowes and Aftalion, 1991; Beard et al., 1995; Jelínek et al., 1997; Zulauf, 1997b; Faryad, 2012). The protolith ages of these rocks show two distinct age groups, ~540 Ma for amphibolites and retrogressed eclogites (Timmermann et al., 2004) and ~496 Ma for gabbro intrusions (Bowes and Aftalion, 1991; Timmermann et al., 2004) occurring along the contact with TCC. The age of the eclogite facies metamorphism (reaching up to 25 kbar and 670°C; Štědrá, 2001; Medaris et al., 2005; Faryad, 2012) remains controversial (see discussion in Timmermann et al., 2004) in contrast to the well-defined amphibolite facies overprint (600–780°C and 9–12 kbar; Jelínek et al., 1997; Štědrá, 2001; Medaris et al., 2011) dated to 380–370 Ma by both Ar/Ar and U/Pb geochronology methods (Dallmeyer and Urban, 1998; Timmermann et al., 2004). Eclogites are restricted to the central part of the MLC, where they occur as boudins and lenticular bodies up to 3.5 km long enclosed by rutile-garnet amphibolite (Fig. 12). Most eclogites are quartz bearing and some contain kyanite. Typical accessory minerals are rutile, ilmenite, and apatite. Most eclogites show an affinity to MORB-type basalts (Kastl and Tonika, 1984; Beard et al., 1995), but some reflect a subduction or oceanic island-basalt component in their source (Beard et al., 1995).

The structural record in the Mariánské Lázně Complex (MLC) is very complex, therefore only limited amount of information have been published. One of the few studies point to the common prolate strain of the kyanite pseudomorphs and interpret gently to moderately SE dipping lineation as a result of constrictional strain due to slab pull in the subduction zone (Zulauf, 1997a). More recent study of Hrouda et al. (2014) subdivided the MLC rocks into two basic structural types: (1) rock with well-developed metamorphic foliation; and (2) massive rock without macroscopically observable fabric elements. In addition, (3) massive rock surrounded by well foliated rock can be locally observed on locality scale (Fig. 13a). The fabric type (1) is developed in banded to laminated amphibolite whose outcrops show well defined metamorphic foliation and often also mineral lineation observable on sample scale. The type (2) is represented by massive amphibolite, often rich in garnet, metagabbro, or gabbro-amphibolite. The metamorphic foliation is either absent or can be identified only on locality scale. In the type (3), the

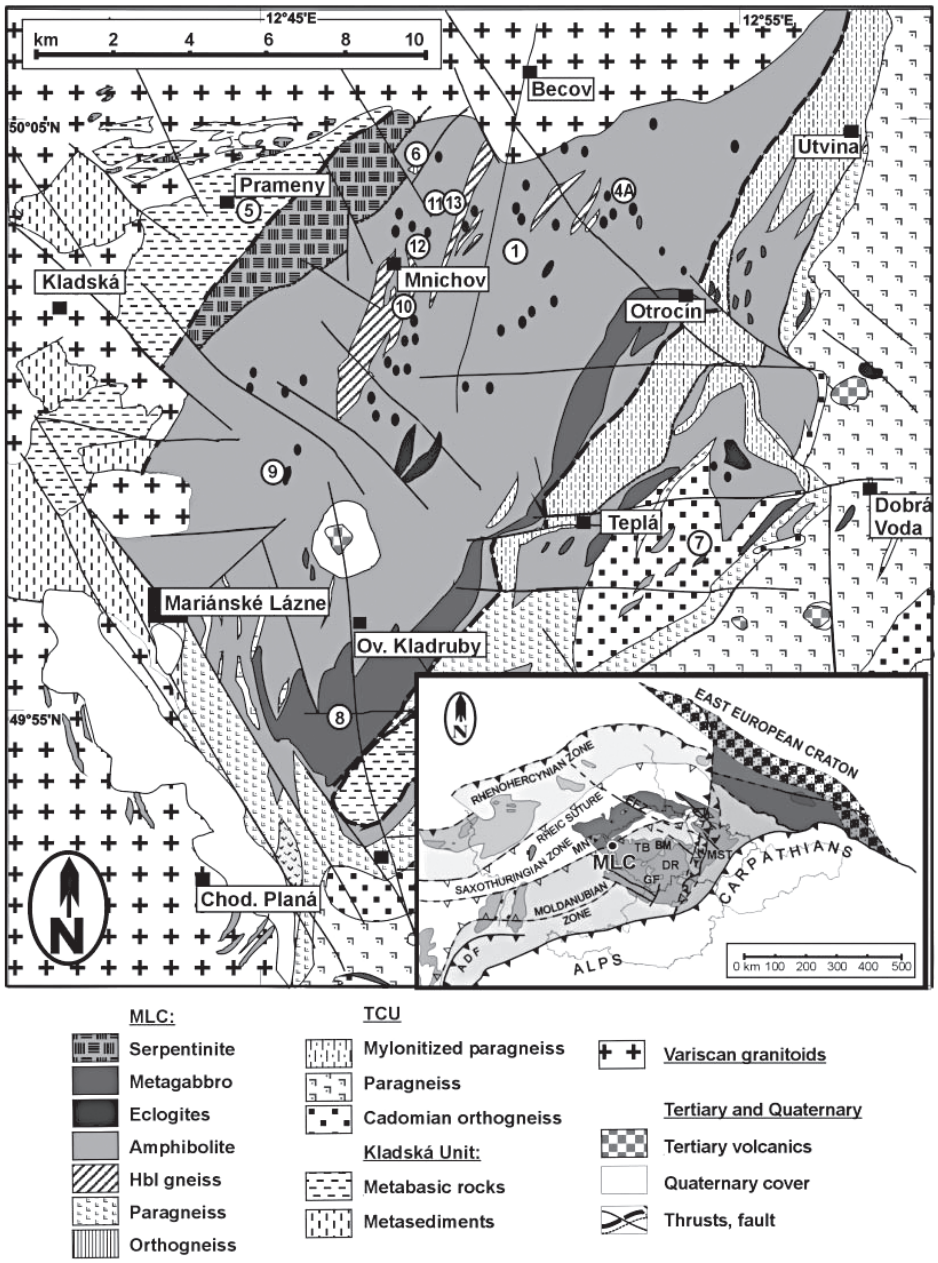

Fig. 12: Schematic geological map of the Mariánské Lázně Complex (Timmermann et al., 2004).

massive rock is represented by amphibolite or to various degrees retrogressed eclogite, which is surrounded by banded amphibolite and/or amphibolite migmatite.

The dominating fabric element in the MLC is metamorphic foliation, which is best developed in the banded to laminated amphibolite originated in the upper amphibolite to granulite facies. This foliation is defined by alternating felsic bands formed by feldspar and quartz, and mafic bands formed by amphibole, subordinate biotite and chlorite with admixtures of quartz and feldspars. The metamorphic foliation hosts a lineation, usually classified as stretching lineation defined by dimensionally oriented aggregates of quartz, feldspar, and amphibole. Migmatitic fabrics and evidence for partial melting in amphibolite were locally observed in the vicinity of the massive retrogressed eclogite lenses. The migmatitic fabrics are usually steep showing various trends ranging from SE–NW to E–W. These fabrics are reworked (sheared and/or folded) by the dominating amphibolite facies metamorphic foliation, which throughout the MLC is gently to moderately dipping towards E, NE or SE. The lineation associated with the latter fabric plunges generally to E–SE. The orientations of the amphibolite metamorphic foliation poles tend to create a wide and irregular partial girdle oriented NNW–SSE and moderately plunging WNW.

METAGABBROS AT THE TCC-MLC BOUNDARY

Coronitic metagabbroic rocks represent specific lithology occurring along the contact between the Mariánské Lázně and the Teplá Crystalline complexes. In the Mariánské Lázně Complex these rocks form a relatively wide belt

bordering the contact with the Teplá Crystalline Complex, in which gabbroic rocks occur as small isolated bodies in the vicinity of the contact zone. The metagabbroids have often well preserved magmatic mineral assemblages and textures containing plagioclase, clinopyroxene, amphibole, orthopyroxene, ilmenite ± biotite, olivine, quartz and spinel (e.g. Jelínek et al., 1997; Kachlík, 1997; Štědrá et al., 2002; Faryad, 2012). Variations in their primary magmatic texture and/or mineral assemblage led Štědrá et al. (2002) to distinguish three groups of metagabbroids in this area: 1) metagabbros – coarse grained rocks with rather simple mineral assemblage of Cpx, Plg, Ilm, Ap ± Ol, Opx, Amp; 2) metadolerites – medium to fine-grained rocks with magmatic mineral assemblage of Plg, Opx, Cpx, Amp, Ilm; and 3) porphyritic metagabbros – porphyritic rocks with Plg phenocrysts in a matrix of Plg, Cpx, Amp, Bt. Metamorphism of these rocks is reflected mostly by formation of various coronas (or their sequence) and partial recrystallization. The bodies of metagabbroids are heterogeneously overprinted by deformation zones affecting their edges as well as their interiors. These zones are characterized by complete recrystallization of the original magmatic texture into amphibolite.

Geochemistry

Detailed geochemical characterization of the metagabbros was provided by Crowley et al. (2002) and Štědrá et al. (2002). These authors show that most of the metagabbroids follow tholeiitic trend in the FeO/MgO vs. TiO_2 discrimination diagram. Based on their chemistry and magmatic mineral assemblage, these rocks can be divided into five groups: 1) Cpx-Opx-Plg-Ol-Ilm-Ap bearing metagabbros with relative enrichment in Mg and Nb and depletion in Ti and REE contents; 2) Cpx-Plg-Ilm-Ap metagabbros enriched in Ti, Eu, Gd and Th and depleted in Rb, Zr, Nb, Ce, Ho and Er; 3) Plg-Cpx-Ilm-Ap metagabbros enriched in alkalis, Ti, Zr, Al, REE, Sr and Si and depleted in Mg and Pr; 4) Opx-Cpx-Plg-Ilm metagabbros enriched in Zr, La, Ce, HREE and deleted in Mg; and 5) Cpx-Opx-Plg-Bt-Hbl metagabbros enriched in Rb, Zr, K, Ba, Pb, Nd, Y, Cr, REE and depleted in Mg, Pr and Er.

Based on their trace element signatures and with the help of the previously published data on isotopic compositions (Beard et al., 1995), Štědrá et al. (2002) concluded that a source of these rocks is of intra-plate sub-continental character rather than that of a mid-ocean ridge. Geochemical characterization of metagabbros from other localities provided by Timmermann et al. (2004) show similarities with E-MORB and calc-alkaline volcanic rocks from Andes (Hickey et al., 1986) with increased Sr and decreased HFSE contents. They concluded that the composition of these metagabbros may indicate a mid-ocean ridge source.

Metamorphic record in the metagabbros

Metamorphism of gabbros is reflected mostly by formation of various coronas or their sequence around the primary magmatic minerals and their partial to complete replacement. This replacement is often static with no apparent deformation-related changes in microstructure. Štědrá et al. (2002) and Faryad (2012) describe following features connected with the metamorphism of the gabbros: Amp and Grt corona formation at the contact of Cpx, Opx, Ilm with Plg; Opx ± Grt around Ol; Opx + Plg symplectite ± Amp around Opx; and recrystallization of magmatic Plg resulting into formation of fine-grained mixture of Plg, Zo, Ky, Bt, Amp and being occasionally accompanied by growth of euhedral Grt grains in the

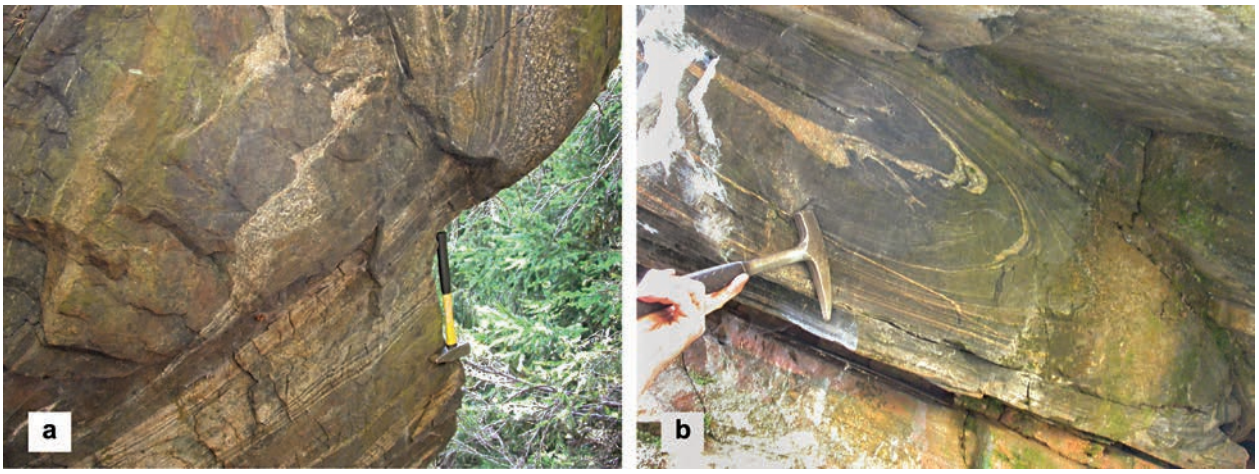

Fig. 13: Sub-vertical deformation fabrics reworked by subhorizontal amphibolite facies fabric in MLC. a) Eclogite lens surrounded by sub-vertical migmatitic fabric to the right and solid state amphibolite-facies fabric below the lens. Note the continuity but distinct appearance of the two fabrics related to subhorizontal shearing. b) Reworking of sub-vertical fabric by isoclinal fold and subhorizontal axial planar cleavage.

Plg domains. In addition, the metagabbro bodies are heterogeneously overprinted by deformation zones affecting their edges as well as their interiors. These zones are characterized by complete recrystallization of the original magmatic minerals into amphibolite (Hbl + Plg) and/or greenschist (Ac + Plg + Zo + Chl).

The metamorphic PT conditions of the metagabbros from the Mariánské Lázně Complex were estimated by several authors (Jelínek et al., 1997; Štědrá et al., 2002; Faryad, 2012) within the range of 585–730 °C and 8–13 kbar. Our preliminary results calculated by using the average PT calculation mode in THERMOCALC (Powell et al., 1998; 2009 version) show that the PT conditions reached by selected samples from the TCC (560–615°C and 8–10.5 kbar) are generally lower compared to PT conditions obtained from metagabbro samples in

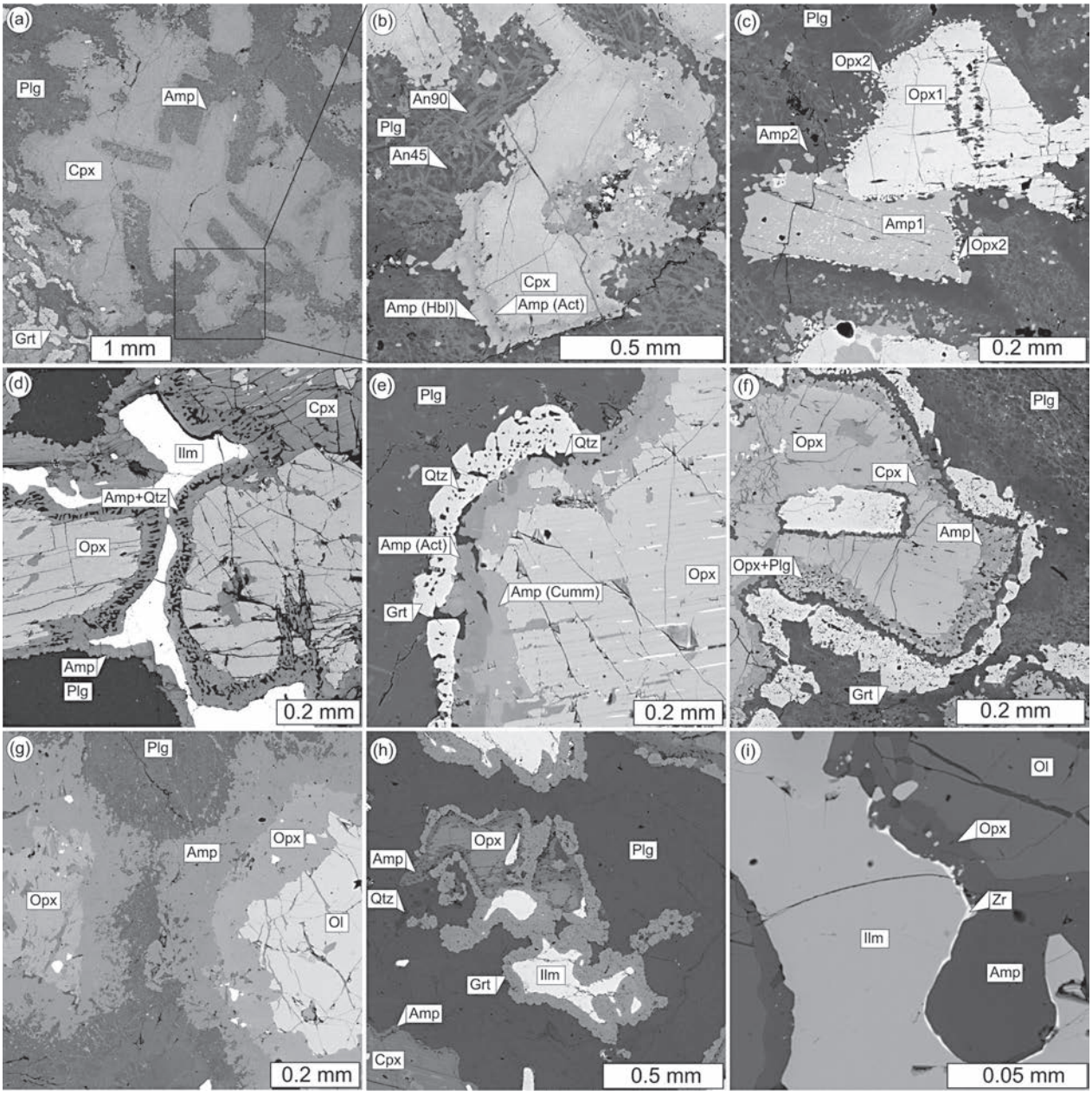

Fig. 14: Main features of the coronitic metagabbros observed in representative samples from the TCC – MLC boundary: a) Poikiloblast of Cpx with Plg inclusions with developed Amp corona in places followed by Grt. b) Detail from a) Plg recrystallized to a mixture of anorthite and andesine, Amp corona with pronounced zoning from Act to Hbl composition. c) Primary Amp1 and Opx1 surrounded by symplectite of metamorphic Opx2+Plg and Amp2. d) Corona of Amp+Qtz symplectite formed along boundaries of primary Opx, Cpx, Plg, and Ilm. e) Multiple corona around magmatic Opx (towards Plg): Amp (cummingtonite), Amp (hornblende)+Qtz, Grt+Qtz. f) Multiple corona around magmatic Opx (towards Plg): Amp (hornblende)+Cpx, Opx2+Plg symplectite, Plg, Grt. g) Typical corona sequence around Ol – Opx followed by Amp. h) Grt corona formed preferentially around Ilm, Amp corona around Opx and Cpx, occasionally followed by Grt. i) Zircon corona around Ilm.

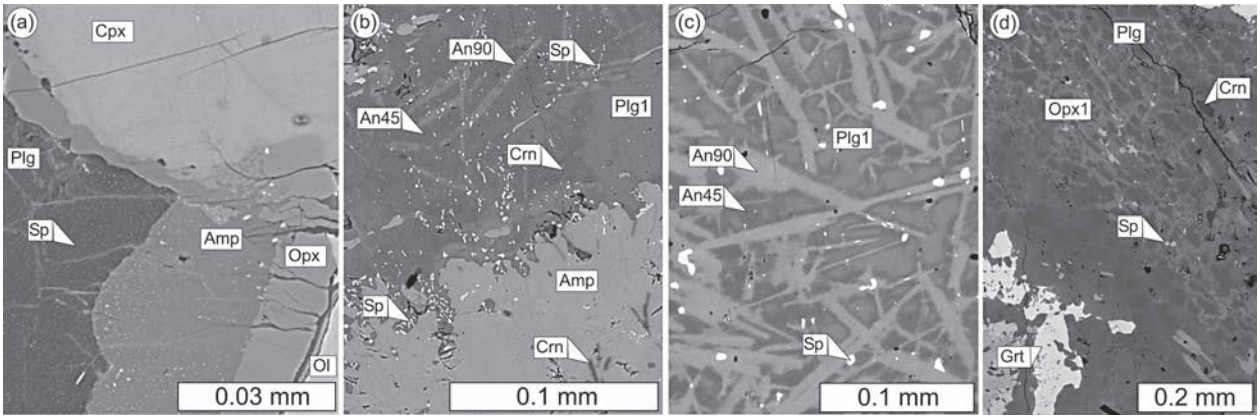

Fig. 15: Progressive break down of Plg during coronitization: a) formation of Sp inclusions inside of Plg. b) Formation of Sp grains and Crn lamellae inside of primary Plg followed by decomposition of Plg1 to two Plg of different compositions – andesine and anorthite. c) Decomposition of Plg1 to two Plg of different compositions – andesine and anorthite. d) Complete recrystallization of the magmatic Plg into fine-grained mixture of Plg grains with Ca increasing to their rims.

the MLC (Výškovice locality; 690°C and 12 kbar). This indicates that similarly to the TCC metapelites also the metamorphic grade in metagabbro increases towards W.

In the metagabbros within TCC, the deformation-related metamorphism presumably in amphibolite to greenschist facies conditions may be related to the M_3 metamorphic event observed in the surrounded metapelitic rocks of the TCC. However it is generally problematic to link the coronitization of these rocks to any of the observed events due to the lack of metamorphism – deformation relationships connected with this process.

General characterization of the coronitic metagabbros from TCC/MLC boundary

Metagabbros present in form large belt along the TCC-MLC boundary and small bodies scattered inside of both units nearby the border show variable metamorphic and textural characteristics with respect to their magmatic mineral assemblage and degree of metamorphism. Magmatic mineral assemblages and microstructures in the metagabbros are generally well preserved. They are characterized by the presence of Plg (labradorite), Cpx (diopside to augite), Opx (enstatite), Amp (edenite to pargasite), Bt, Ilm and Sp, some samples additionally contain primary Ol or Qtz.

Metamorphism is mainly reflected by formation of single or multiple coronas at the contact of Plg and other primary magmatic minerals. Following coronas or their sequences in direction towards Plg can be observed: Cpx is surrounded either by no corona, or by narrow layer of Amp with Al increasing at the contact with Plg, which may be followed by Grt layer (Fig. 14a, b). Amp can be surrounded by a layer of Opx+Plg symplectite (Fig. 14c). Opx shows high variability in developed coronas with following sequences observed in different samples: 1) Amp ± Qtz (Fig. 14d); 2) alternation of Hbl+Plg and Opx+Plg symplectites (Fig. 14c); 3) Amp (cummingtonite)→Act+Qtz symplectite→Hbl→Grt (Fig. 14e); and 3) Cpx+Hbl→Opx+Plg symplectite→Grt (Fig. 14f). Bt is surrounded by Amp and/or by symplectitic corona of Opx+Sp, occasionally followed by Grt. Ol is always enveloped by double corona of Opx followed by Amp occasionally alternating with Opx+Sp symplectite (Fig. 14g). Ilm is in some samples surrounded by Grt corona (Fig. 14h) but rim defined by zircon layer or tiny zircon grains can be observed in all studied lithologies (Fig. 14i). Following features appear with respect to the primary magmatic mineral assemblage: 1) Grt coronas are developed only in Ol-free samples, 2) Qtz is a part of Act+Qtz symplectites in sample with primary Qtz only.

In addition, progressive breakdown of the original magmatic Plg can be observed based on the studied sample sequence: 1. crystallization of small spinel grains and corundum lamellae in the Plg indicating Ca>Al diffusion from Plg accompanied by Mg+Fe diffusion into Plg (Fig. 15a & b); 2. breakdown of the magmatic Plg (labradorite) to andesine (An = 45%) and anorthite (An = 90%; Fig. 15b & c); and 3. recrystallization of the magmatic plagioclase into fine-grained clusters of zoned Plg grains (increase of Ca to rims) accompanied with Sp, Ky and Crn (Fig. 15d).

Field trip programme

The above mentioned tectonic evolution will be discussed along a profile with 5 stops running across the contact between the Teplá Crystalline Complex (TCC) and the underlying Mariánské Lázně Complex (MLC). The profile is characterized by a consecutive increase in metamorphic grade from structurally uppermost Stop 1 to structurally lowermost Stop 5.

The associated differences in deformation history and change in structural styles at different crustal depths will be demonstrated (Figs. 16 & 17).

Along the profile, four principal belts with distinct lithology and/or tectono-metamorphic evolution can be distinguished (Figs. 16 & 17). These are: i) phyllite belt covering biotite and garnet zone in the TCC; ii) micaschist belt covering staurolite and kyanite zone in the TCC; iii) metagabbro belt comprising mostly of coronitic metagabbros in the MLC; and iv) eclogite belt characterized by occurrence of eclogite lenses in the host amphibolite migmatite in the MLC. Associated structural record is represented by a repeated sequence of two structural styles, i.e. pattern A characteristic for the phyllite and metagabbro belts and showing dominant sub-vertical fabric S_2, and pattern B characteristic for the micaschist and eclogite belts and showing dominant gently inclined fabric S_3 (Fig. 18).

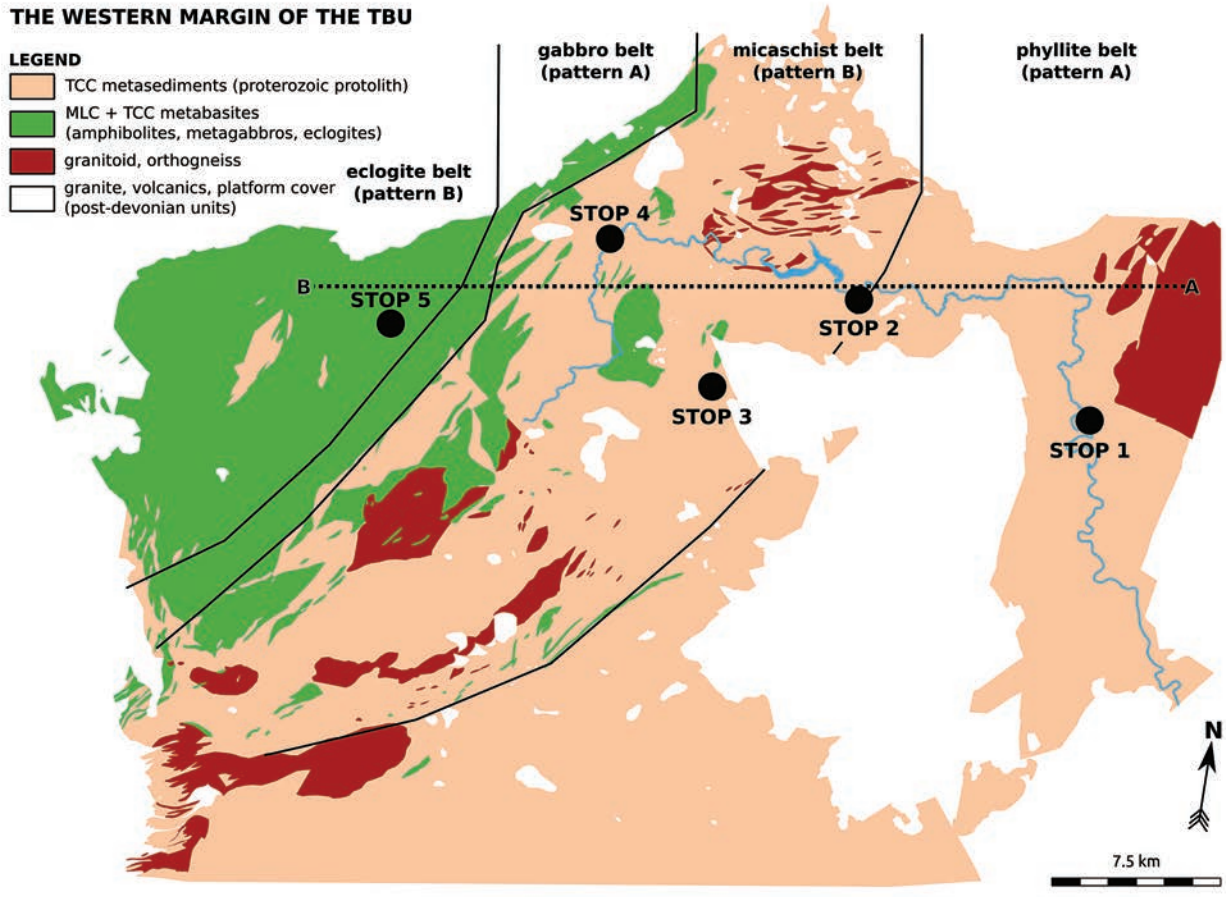

Fig. 16: Simplified geological map of the western margin of the Teplá Barrandian Unit. The field trip Stops are shown with respect to the position of the four structural domains. The A-B line shows location of the geological profile in figure 17.

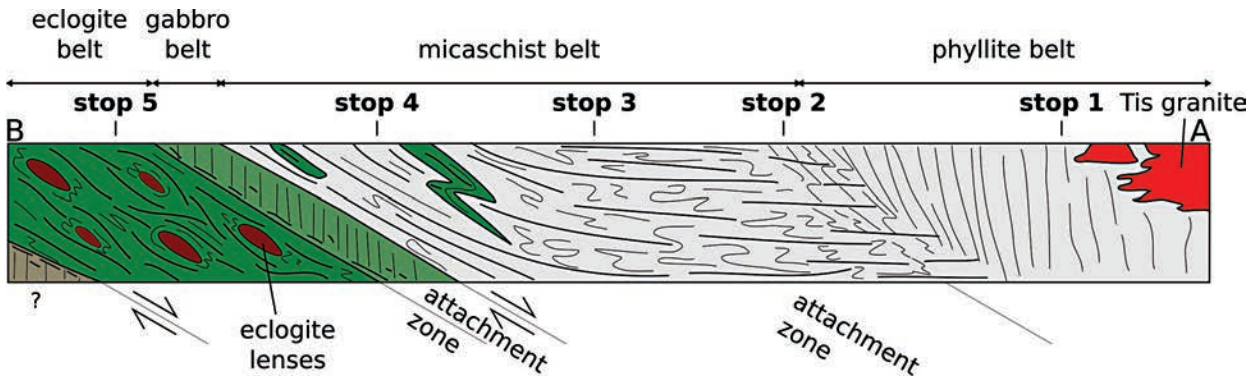

Fig. 17: Geological profile across the contact between the Mariánské Lázně Complex and Teplá Crystalline Complex.

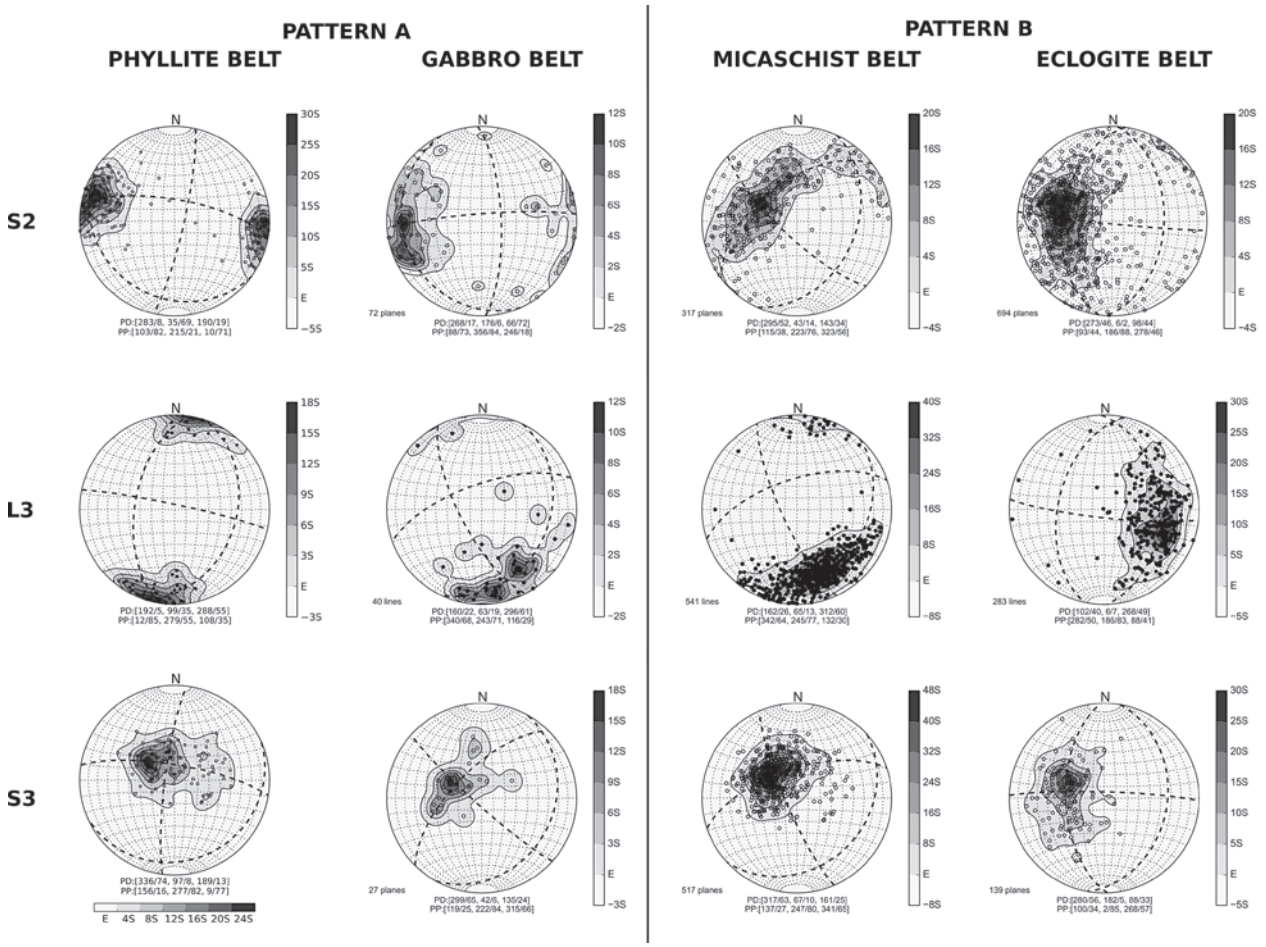

Fig. 18: Structural data characteristic for the two structural patterns A and B, respectively. Pattern A occurs in the phyllite and metagabbro belts and is characterized by dominant N–S trending vertical fabric S_2. Pattern B occurs in the micaschist and eclogite belts and is characterized by the transposition of S_2 to gently inclined S_3 fabric and rotation of lineation L_3 towards the E-dipping attractor.

Stop 1 – Rabštejn phyllite

GPS coordinates: 50.0472122N, 13.2937711E
Position: eastern phyllite belt
Metamorphic grade: biotite zone
Structural style: D_2 dominated domain

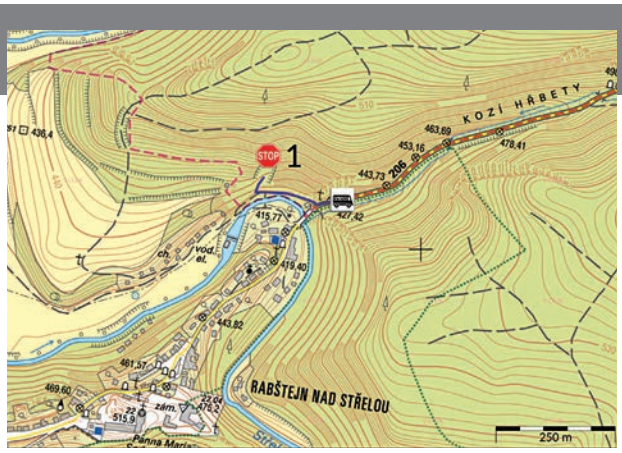

This Stop is located in the very east of the excursion profile i.e. in the uppermost structural level (Fig. 16). Here the low-grade chlorite-sericite to biotite bearing phyllites are exposed. The outcrop is dominated by a sub-vertical N-S trending cleavage S_2 (Fig. 19b) overprinting a subhorizontal bedding-parallel foliation S_{0-1} (Fig. 19a & f). Based on the correlation of deformation structures and their typical metamorphic-geochronological record in the surrounding area the S_2 is interpreted to be of the early Variscan age while S_{0-1} is probably of Ordovician age. At the outcrop it is possible to identify two end member cases of the transposition: 1) zones of complete transposition of S_1 to S_2 (Fig. 19j) and 2) S_2 low-strain domains manifested by hinge zones of meter-scale open to closed F_2 folds with gently southward-plunging axes (Fig. 19g). In addition, this outcrop also shows incipient D_3 shortening demonstrated by kink-bands with gently west-dipping axial planes S_3 and crenulations with subhorizontal axial planes and subhorizontal crenulation lineation L_3 on the sub-vertical S_2 planes (Fig. 19d,e & j).

The metamorphic record at this stop is indicative of biotite zone that mostly corresponds to the M_1 metamorphic event manifested by mineral assemblage of muscovite, biotite, quartz, plagioclase and ilmenite (Fig. 19f). There are usually no newly grown minerals associated with the S_2 cleavage in this area (Fig. 19h). On the other hand towards the west and in the intensely transposed domains of S_2 cleavage, the M_2 mineral assemblage of Ms + Bt + Plg + Qr + Grt + Ilm can be identified (Fig. 19i).

The most important mineral phase of the M_2 assemblage in the surrounding area is garnet with its first occurrence only several hundred meters to the west from Stop 1. From this point and further to the west, garnet becomes stable member of the M_2 assemblage. The thermodynamic modelling of PT conditions associated with the first occurrence of M_2 garnet (Fig. 19h) revealed PT conditions of ~540°C at 6 kbar. D_3 deformation in the phyllite belt is very weak, the associated M_3 metamorphic metamorphism is revealed by replacement of euhedral garnet by chlorite and/or by growth of large randomly oriented chlorite porphyroblasts (Fig. 19i).

The Variscan age of S_2 cleavage in the studied region is further documented by two lines of evidence: 1) The Tis granite represents a sill that was emplaced into the subhorizontal S_{0-1} anisotropy at 505 Ma (Venera et al., 2000) and its margins are overprinted by solid-state mylonitic S_2 fabric. 2) The Ar/Ar data on micas from the nearby Chyše cliffs yielded an age of ~375 Ma (Dallmeyer and Urban, 1998).

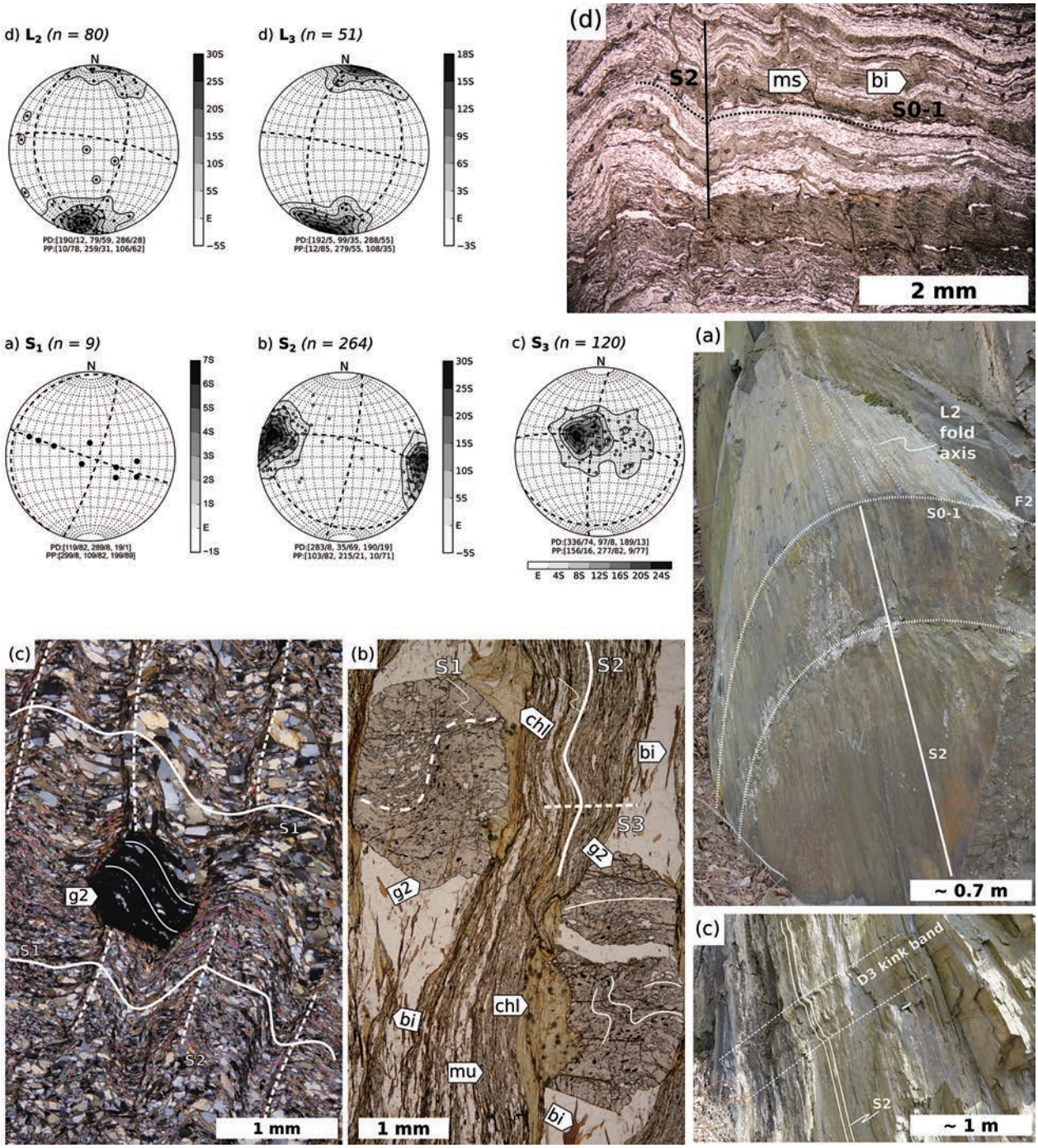

Fig. 19: Structural and metamorphic record in the phyllite belt. a) S_1 foliation forms a girdle due to superposed deformation D_2; b) subvertical cleavage S_2; c) fold axes and intersection lineation L_2; d) crenulation lineation L_3 and axes of kink bands; e) axial planes of kink bands and crenulations S_3; f) microphotograph of the hinge domain of F_2 folds, bedding parallel foliation S_{0-1} form major anisotropy, which is folded during D_2 deformation; g) meter-scale closed fold F_2 in the D_2 low-strain domain from Stop 1; h) first occurrence of garnet in the phyllite belt, note folded inclusion trails inside garnet porphyroblast suggesting its syn-D_2 growth; i) complete transposition of S_1 foliation to sub-vertical S_2 foliation and complete replacement of M_1 by M_2 assemblage (garnet, muscovite, biotite), chlorite replacing garnet is subsequent to M_2 i.e. related to M_3 event; and j) D_2 high strain domain at Stop 1 shows complete transposition of S_1 to S_2 cleavage, which is overprinted by D_3 kink bands.

Stop 2 – Žlutice cliffs

GPS coordinates: 50.0808472N, 13.1417331E
Position: phyllite/micaschist belt boundary zone
Metamorphic grade: staurolite isograd
Structural record: transitional domain D_2\D_3 superposition

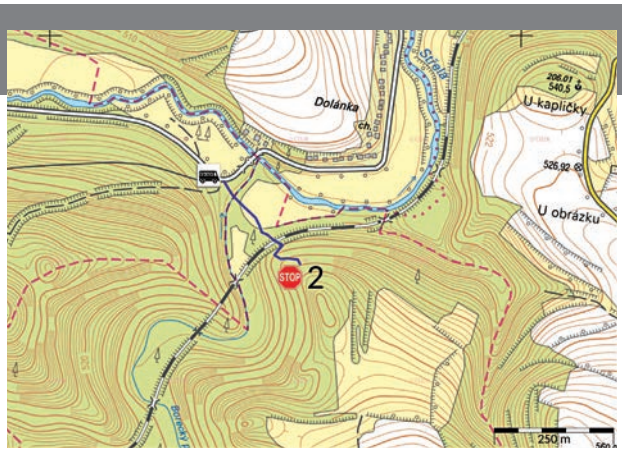

Stop 2 is located near the transition between phyllite and micaschist belt (Fig. 16). In contrast to the previous stop, the dominant S_2 foliation at this locality is strongly affected by D_3 deformation event (Fig. 20a-c). D_3 event is associated with sub-vertical shortening reflected by F_3 folds with subhorizontal axial planes and local development of axial planar cleavage. Closed F_3 folds have SSW-NNE trending axes (Fig. 20b). Numerous F_3 folds affect the primary pelite-wacke alternations securing the easy recognition of these folds in the field (Fig. 20d-g). The original sedimentary stratification also provides a great opportunity to demonstrate the effect of a layer competence on the intensity of S_3 cleavage, i.e. S_3 cleavage is well developed in metapelites, whereas S_2 is dominating in metagreywackes.

As S_2 foliation is the dominant deformation fabric in this area, the metamorphic record is reflected by the M_2 mineral assemblage comprising of muscovite, biotite, garnet, quartz, plagioclase and ilmenite (Fig. 20i). The very first occurrence of staurolite, marking the staurolite isograd, was revealed in a thin section from an outcrop just across the creek to the north from Stop 2 (Fig. 20h). The peak PT conditions reached during the M_2 event by the surrounding rocks were estimated to ~580°C at 7 kbar. The retrogression during the M_3 event is documented by replacement of garnet by biotite and by growth of chlorite porphyroblasts.

In-situ monazite LA-ICPMS U/Pb dating was performed in a sample close to this locality. All of the analyzed monazites belong to the same age group with an age of 375 ± 3 Ma. It is very likely that this age is associated with the M_2 mineral assemblage as two of the analyzed monazites came from the garnet 2 core. Similar age of 375 ± 1 Ma obtained from nearby locality by Ar/Ar technique on muscovite (Dallmeyer and Urban, 1998) suggests that peak M_2 metamorphism and subsequent M_3 retrogression to temperatures below blocking temperature for the Ar/Ar in muscovite must happened very close.

Fig. 20: Typical deformation-metamorphic features at Stop 2 – Žlutice cliffs. a) S_2 girdle with common π-pole plunging gently to the SSW; b) subhorizontal S_3 cleavage and fold axial planes; c) fold axes L_3; d) asymmetric fold F_3 with well-developed cleavage S_3 in the metapelite and S_2 mimicking bedding in the adjacent metagreywacke; e) detail of the S_3 cleavage in the hinge zone of F_3 fold; f) moderately ESE dipping limb of F_3 fold and associated cleavage; g) closed symmetrical F_3 folds in the metagreywackes; h) first staurolite porphyroblast in the micaschist below Žlutice cliffs, large chlorite porphyroblast is related to M_3 retrogression event; and i) garnet bearing foliation S_2 in a metapelite.

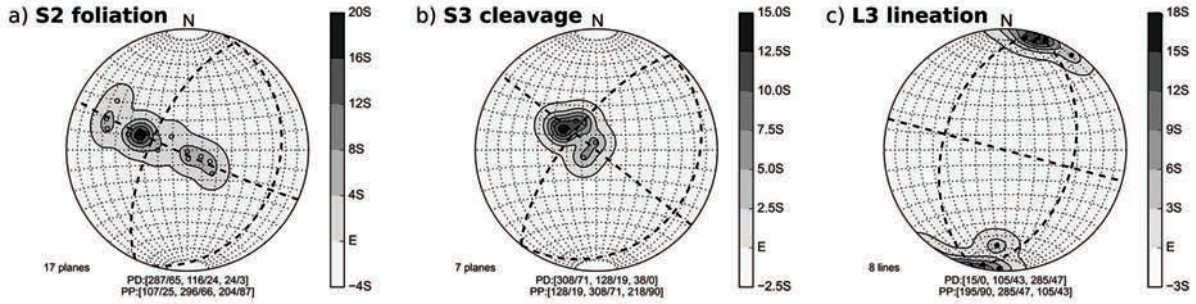
a) S2 foliation
N
20S
16S
12S
8S
4S
E
−4S
17 planes
PD:[287/65, 116/24, 24/3]
PP:[107/25, 296/66, 204/87]
b) S3 cleavage
N
15.0S
12.5S
10.0S
7.5S
5.0S
2.5S
E
−2.5S
7 planes
PD:[308/71, 128/19, 38/0]
PP:[128/19, 308/71, 218/90]
c) L3 lineation
N
18S
15S
12S
9S
6S
3S
E
−3S
8 lines
PD:[15/0, 105/43, 285/47]
PP:[195/90, 285/47, 105/43]

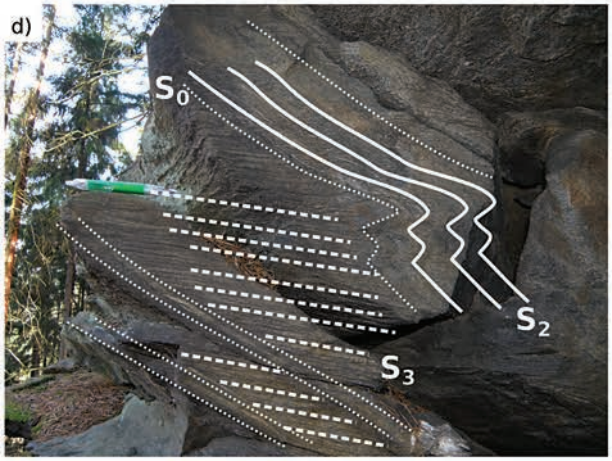
d)
S0
S2
S3


e)
S2


f)
S0
S2
S3
10 cm

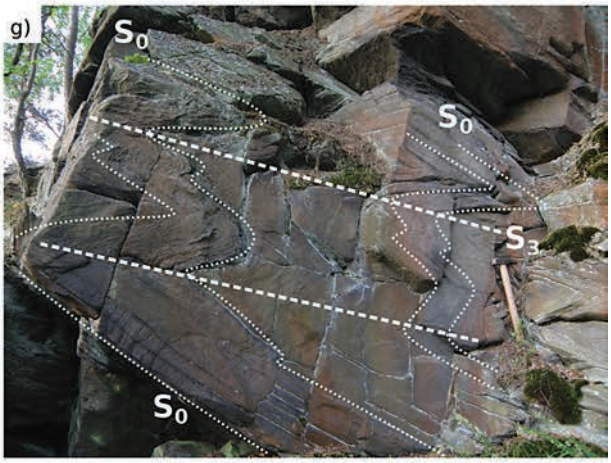
g)
S0
S0
S3
S0

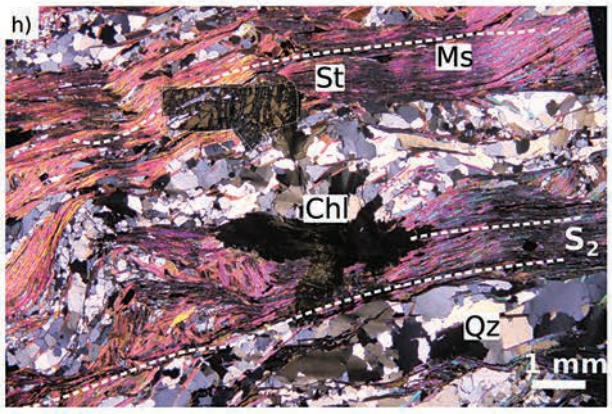
h)
Ms
St
Chl
S2
Qz
1 mm

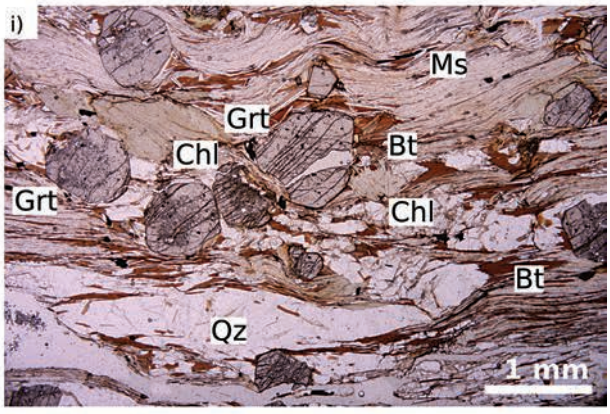
i)
Ms
Grt
Chl
Bt
Grt
Chl
Bt
Qz
1 mm

Stop 3 – Komárov micaschist

GPS coordinates: 50.0375961N, 13.0604303E
Position: micaschist belt
Metamorphic grade: staurolite zone
Structural record: D_3 dominated domain

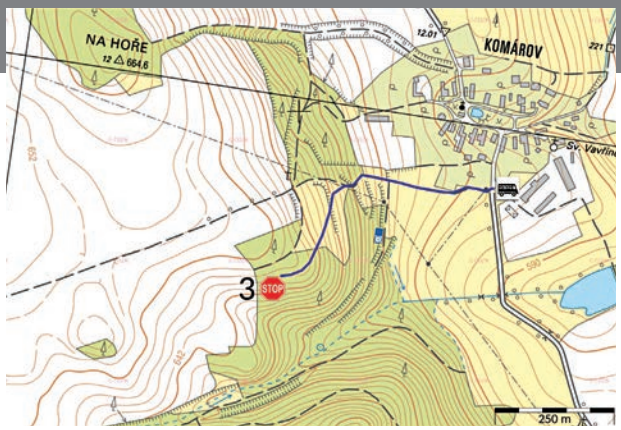

The Stop 3 in the TCC metasediments is situated in the staurolite zone of the micaschist belt. The structural record in the micaschist belt differs significantly from that of the phyllite belt mainly due to an intense D_3 transposition and evidence for F_3 isoclinal folds. Most of the outcrops in the micaschist belt are dominated by gently inclined fabric and it is often difficult to distinguish between the S_2 preserved in the limbs of F_3 folds and the newly developed cleavage S_3 (Fig. 21a-e). The outcrop at Stop 2 is situated in the hinge zone of a large-scale F_3 fold, where D_3 overprint is not so strong and therefore the relationship between S_2 and S_3 can be observed (Fig. 21e & j). Detailed observation of the outcrop reveal that principal stretching direction of D_3 is approximately east-west and gently eastward plunging. This suggests a progressive redistribution of lineation from its initial intersection N-S orientation, typical for D_3 low strain domains, towards the D_3 east plunging attractor in the intensely sheared rocks. As the intensity of D_3 generally increases towards the west, lineation in the micaschist belt creates a girdle spreading from gently south-plunging to gently east-plunging orientations (Fig. 21f). Despite the generally continual rotation of lineation from east to west, some outcrops including Stop 3 provide the opportunity to observe distinct orientations of fold axes and lineation even at a single outcrop (Fig. 21i).

The mineral assemblage related to S_2 fabric consists of muscovite, biotite, quartz, plagioclase garnet and staurolite (Fig. 21k). M_2 minerals are strongly aligned and folded by F_3 folds. Retrogression of the M_2 assemblage is weak at this stop and again includes breakdown of garnet and staurolite in favor of biotite and chlorite. Phase equilibrium modelling of the M_2 assemblage from nearby locality revealed prograde PT path starting at ~480°C and 6.5 kbar, consistent with zoisite and paragonite inclusions preserved in the garnet core, and leading to ~650°C and 7 kbar, documented by kyanite+staurolite+plagioclase polyphase inclusions in the garnet rim. Despite the fact that this locality only contains staurolite in the matrix, the rocks probably reached kyanite stability field.

Fig. 21: Micaschist belt – Komárov micaschist: a-e) structural record in the western domain and the problematics of large scale isoclinal folding in deciphering fabric, hinge domains usually have strong lineation (prolate domains), while lineation in the fold limbs is usually weak (oblate domains); f) summarized stereoplot for the L_3 in the western domain, note that L_3 is ca. 45° rotated compared to L_3 in the eastern domain; g) as a result of F_3 folding, S_2 forms a girdle with common π-pole (PI) corresponding to L_3 lineation in the area; h) gently to moderately SE dipping cleavage S_3 in the western domain; and i) structural data from the Komárov outcrop, note variable orientation of L_3 fold axes.

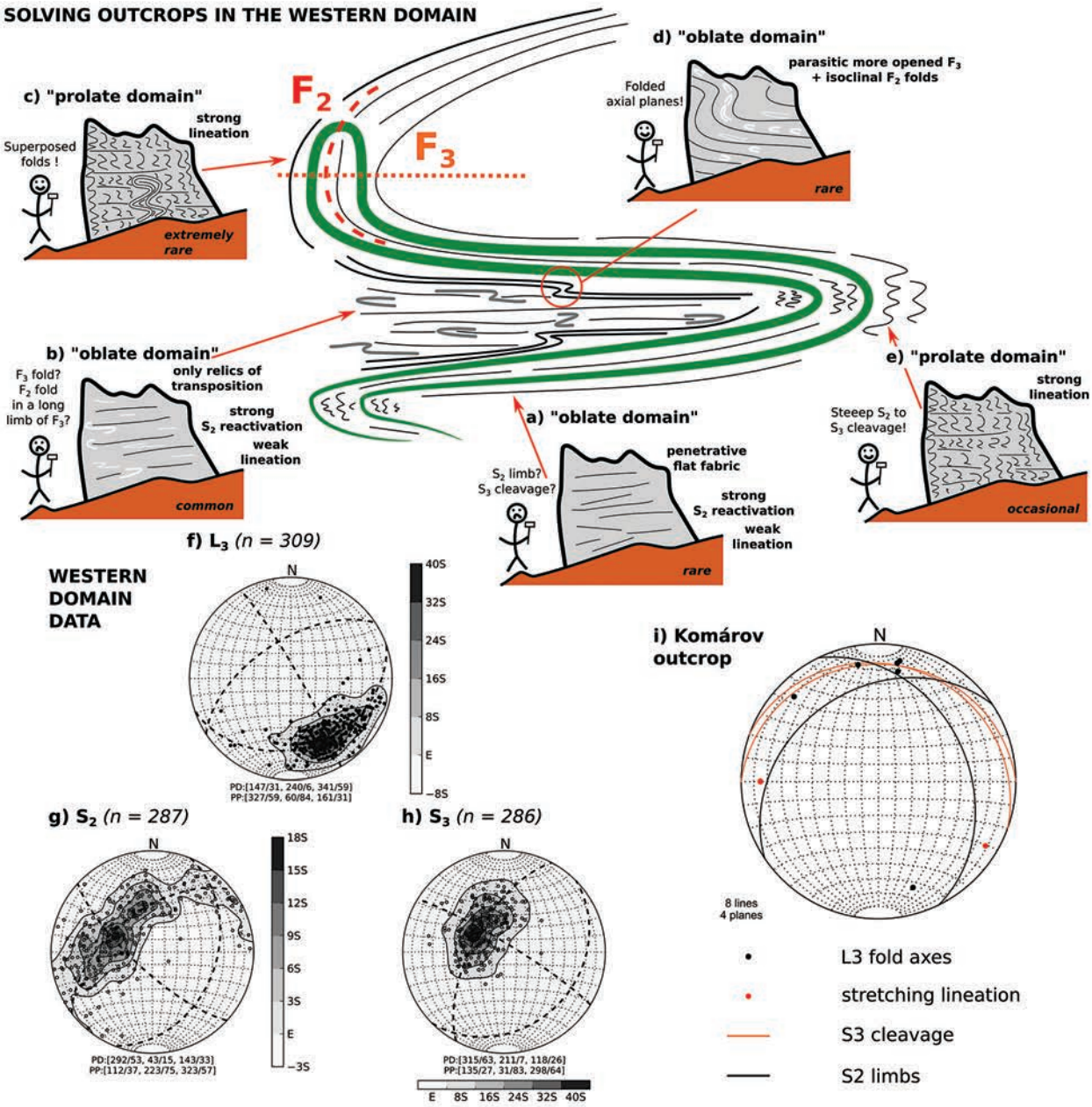
SOLVING OUTCROPS IN THE WESTERN DOMAIN
c) "prolate domain"
Superposed folds !
strong lineation
extremely rare
F2
F3
d) "oblate domain"
Folded axial planes!
parasitic more opened F3 + isoclinal F2 folds
rare
b) "oblate domain"
F3 fold? F2 fold in a long limb of F3?
only relics of transposition
strong S2 reactivation
weak lineation
common
a) "oblate domain"
S2 limb? S3 cleavage?
penetrative flat fabric
strong S2 reactivation
weak lineation
rare
e) "prolate domain"
Steeep S2 to S3 cleavage!
strong lineation
occasional
f) L3 (n = 309)
WESTERN DOMAIN DATA
N
40S
32S
24S
16S
8S
E
8S
PD:[147/31, 240/6, 341/59]
PP:[327/59, 60/84, 161/31]
g) S2 (n = 287)
18S
15S
12S
9S
6S
3S
E
3S
PD:[292/53, 43/15, 143/33]
PP:[112/37, 223/75, 323/57]
h) S3 (n = 286)
PD:[315/63, 211/7, 118/26]
PP:[135/27, 31/83, 298/64]
E 8S 16S 24S 32S 40S
i) Komárov outcrop
8 lines
4 planes
L3 fold axes
stretching lineation
S3 cleavage
S2 limbs

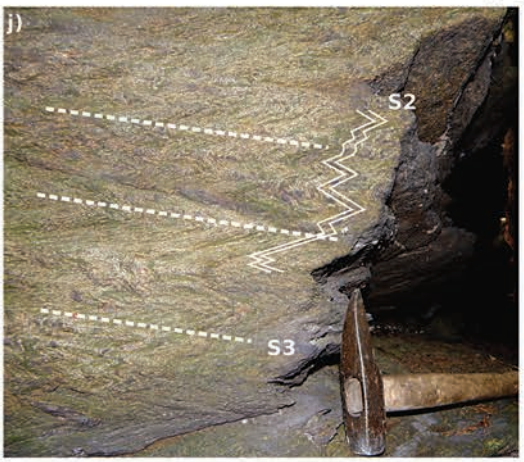
j)
S2
S3

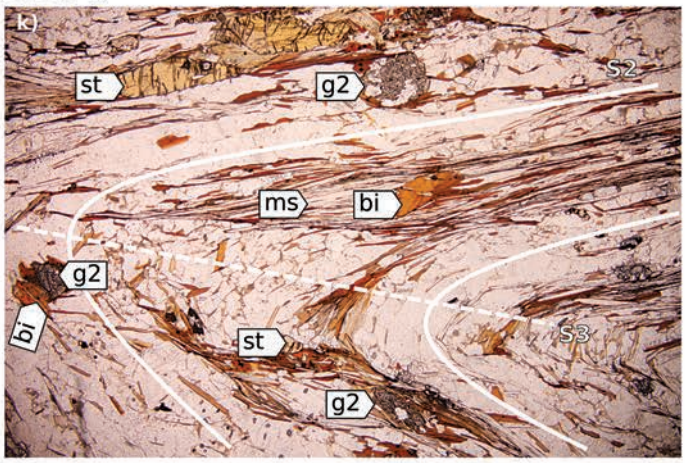
k)
st
g2
S2
ms
bi
g2
bi
st
S3
g2

Stop 4 – Chylice (Malinův) mill metagabbro

GPS coordinates: 50.0896861N, 12.9836733E
Position: micaschist belt
Metamorphic grade: kyanite zone
Structural record: D_2\D_3 dominated domain

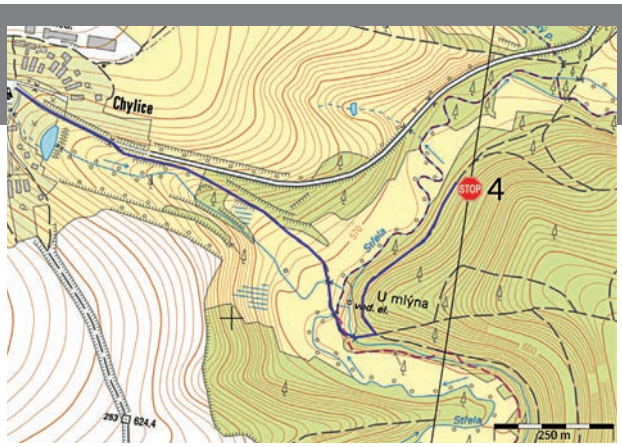

Several tens of meters large body of metagabbro is present within the micaschist belt close to the contact with metabasites of the Mariánské Lázně Complex. Although this area is dominated by deformation fabrics related to D_3, the metagabbro is rather undeformed and its presence is associated with D_3 strain shadows and preservation of steep S_2 fabrics in micaschist in the vicinity of the body. Crenulation lineation L_3 and subhorizontal crenulation cleavage can be observed at outcrops in the vicinity of the gabbro body. The metamorphic grade of M_2 mineral assemblage defining the S_2 fabric in micaschist reaches kyanite zone.

Coronitic metagabbro at this locality (Fig. 22) has well preserved primary magmatic mineral assemblage composed of Ol, Plg, Cpx, Amp, Bt, Opx, and Ilm (Fig. 22a & b). Euhedral Ol grains are represented by compositionally homogeneous forsterite (X_{Mg} = 0.70–0.74), Plg is not systematically zoned but shows large span of compositions from oligoclase to labradorite (An = 18–53 %). Cpx forms euhedral crystals with increasing Ti, Fe and Mg and decreasing Al and Cr from core to rim (X_{Mg} = 0.77–0.80) where the core corresponds to augite and the rim composition corresponds to diopside. Magmatic Amp forms anhedral interstitial grains in between pyroxenes and olivine. Its composition corresponds to edenite/pargasite with Ti decreasing towards the rim. Bt with phlogopite composition (X_{Mg} = 0.80–0.85) as well as Opx (enstatite, X_{Mg} = 0.70–0.78) are rather rare in this rock and form anhedral grains between the Ol, Plg and Cpx. Ilmenite forms anhedral grains that are often associated with Cr-rich spinel and magnetite. Common accessory phases are apatite, pyrhotine, and pentlandite.

Metamorphism of this metagabbro is reflected by formation of single or multiple coronas mostly at the contact of Plg with other phases. Ol (containing characteristic lamellae composed of Mt, Cpx, and Amp) is always surrounded by double corona of Opx (enstatite; X_{Mg} = 0.78–0.78) followed by Amp (pargasite, X_{Mg} = 0.74–0.79) (Fig. 22a–d). In places, Amp layer is alternating with fine-grained-symplectite of Sp + Opx (Fig. 22c & d). On the contrary, Cpx shows no reaction textures at its rims. Seldom Bt is surrounded by a layer of alternating Amp / Sp + Opx symplectite corona (Fig. 22d). Ilmenite is sometimes surrounded by tiny grains of Zr, which is a widespread phenomenon observed in coronitic metagabbros from this area (Fig. 14i). Plg mostly does not show any recrystallization (although it is a common feature at other metagabbro localities), however it often contains very small inclusions of Sp that are organized in rows respecting the Plg crystallography (Fig. 15a). This feature is reflected by so called "clouding" of the Plg resulting in its brown colour in optical microscope and can be attributed to Ca > Al diffusion from the Plg accompanied by Fe+Mg income to Plg from other phases during the corona formation. In several places, irregular spots formed by fine-grained symplectite composed of Zo + Ab + Mu can be observed to replace the magmatic Plg (Fig. 22e & f).

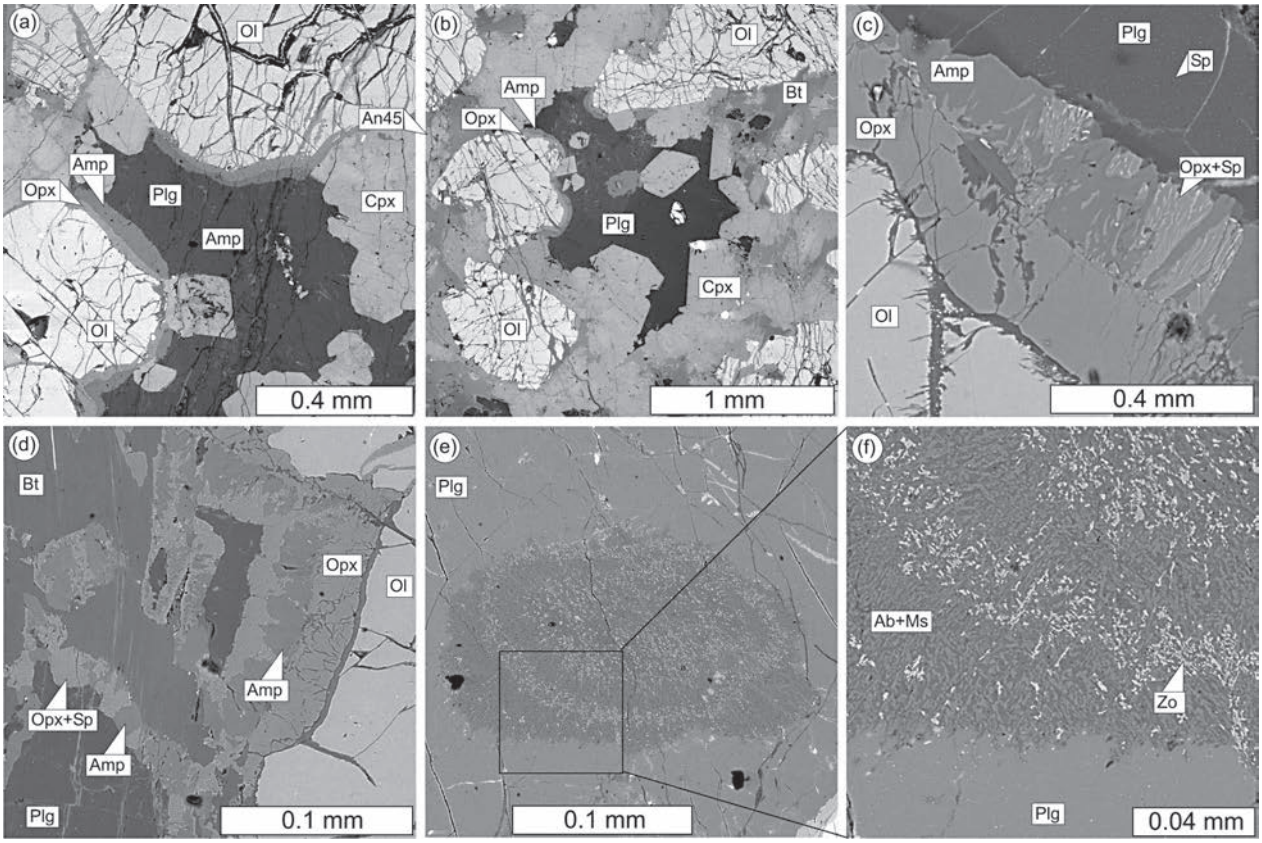

Fig. 22: Characterization of the olivinic metagabbro from the Chylice (Malinův) mill locality. (a–b) Main magmatic mineral assemblage Ol + Cpx + Plg with developed double Opx and Amp corona at the contact Ol with Plg. Note absence of reaction at the Cpx – Plg contact. (c) Detail of the corona at the contact of Ol and Plg: layer of Opx is followed by Amp alternating with Sp + Opx symplectite. (d) Coronas around Ol (Opx followed by Amp alternating with Sp + Opx symplectite) and Bt (Amp alternating with Sp + Opx symplectite, Opx layer is absent). (e–f) Break down of Plg resulting in formation of mixture of Ms + Ab + Zo.

Stop 5 – Tisová metabasites

GPS coordinates: 50.0427089N, 12.8581203E
Position: eclogite belt
Metamorphic grade: eclogite/granulite facies
Structural record: D_3 dominated domain

Stop 5 is located in the metabasites of the eclogite belt. The Structural record at this locality resembles the record of the micaschist belt with the distinction that D_3 reaches even higher strains. The outcrop is dominated by foliated migmatitic amphibolites with fabrics anastomosing around stiff boudins of garnet amphibolites, which bear relics of eclogite facies minerals (Fig. 23b). The main migmatitic foliation S_2 is steep in the D_3 strain shadows preserved in the vicinity of boudins and it is isoclinally folded by F_3 folds with sub-horizontal axial planes away from the shadows suggesting the originally steep orientation of S_2. Away from boudins, S_2 is intensely transposed by axial-planar cleavage S_3, which moderately dips to the SE (Fig. 23a). D_3 is also associated with development of sharp shear zones with well preserved dip-slip lineation L_3 (Fig. 23a). The internal foliation in boudins is usually sub-vertical and shows variable trends although the reason for this variability is not fully resolved (Fig. 23a).

D_3 deformation is associated with intense recrystallization and replacement of the older mineral assemblage, which is best illustrated at boundaries of the boudins (Fig. 23c). The boudins usually have a weak foliation consisting of garnet, amphibole plagioclase and rutile. Towards the shear zone garnet is progressively replaced by symplectites composed of zoisite + amphibole + plagioclase. As the deformation and retrogression of garnet becomes more intense, the equiaxial garnet grains are completely replaced by symplectite which becomes elliptical. In the extreme D_3-M_3 progression, the elliptical symplectites are replaced by penetrative lower-grade amphibolite foliation S_3 defined by amphibole, plagioclase, zoisite and sphene.

The age of migmatization ~375 Ma is well constrained by numerous U/Pb data from melt segregations reported by Timmermann et al. (2004). In addition, similar age is estimated for the formation of S_3 foliation based on K/Ar cooling age of hornblende (Dallmeyer and Urban, 1998).

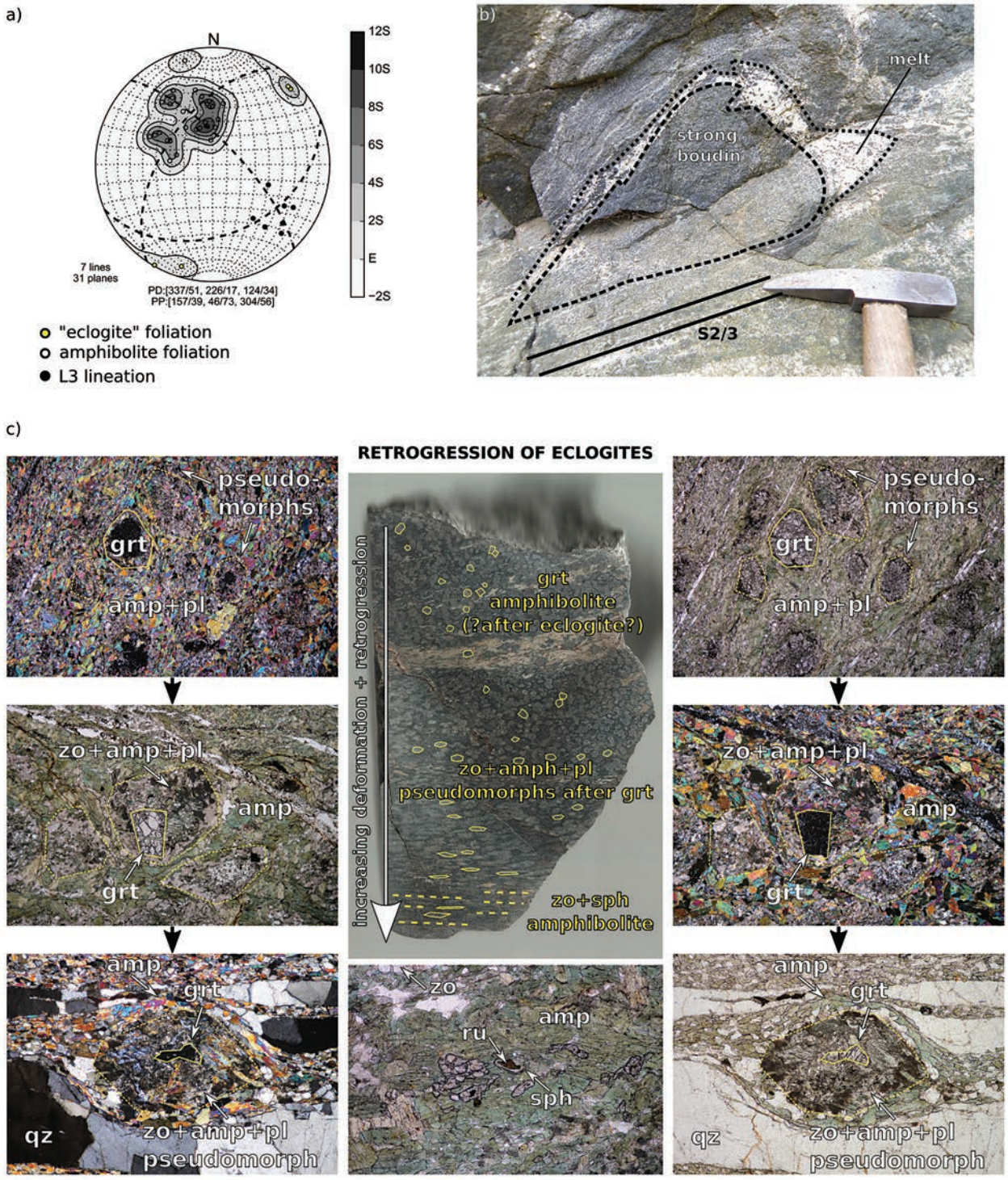

Fig. 23: Structural and metamorphic record in the eclogite belt. (a) Structural data in the Tisová locality, main amphibolite foliation together with foliation in the strong boudins ("eclogite foliation") define a girdle with common π-pole corresponding to L_3 orientation in the area; (b) strong boudin of garnet amphibolite (possibly former eclogite) surrounded by migmatitic amphibolite foliation and with a melt pocket in the D_3 pressure shadow; and c) retrogression of eclogites, for details see text.

References

Beard, B. L., L. G. Medaris, C. M. Johnson, E. Jelínek, J. Tonika, and L. R. Riciputi (1995). Geochronology and geochemistry of eclogites from the Mariánské Lázně Complex, Czech Republic: implications for Variscan orogenesis. *Geologische Rundschau* 84.3, 552–567.

Bowes, D. R. and M. Aftalion (1991). U-Pb zircon isotopic evidence for early Ordovician and late Proterozoic units in the Marianske Lazne complex, Central European Hercynides. *Neues Jahrbuch für Mineralogie* 7, 315–326.

Bowes, D. R., O. Van Breemen, A. M. Hopgood, and E. Jelínek (2002). $^{40}Ar/^{39}Ar$ isotopic evidence for mid-Devonian post-metamorphic pegmatite emplacement in the Mariánské Lázně Complex, Bohemian Massif, Central European Hercynides. *Neues Jahrbuch für Mineralogie-Monatshefte* 10, 445–457.

Crowley, Q. G., P. A. Floyd, V. Štědrá, J. A. Winchester, V. Kachlík, and J. G. Holland (2002). The Mariánské-Lázně Complex, NW Bohemian Massif: development and destruction of an early Palaeozoic seaway.*Geological Society, London, Special Publications* 201.1, 177–195.

Dallmeyer, R. D. and M. Urban (1998). Variscan vs Cadomian tectonothermal activity in northwestern sectors of the Tepla-Barrandian zone, Czech Republic: constraints from 40Ar/39Ar ages. *Geologische Rundschau* 87.1, 94–106.

Dewey, J. F. and K. C. A. Burke (1973). Tibetan, Variscan, and Precambrian basement reactivation: products of continental collision. *The Journal of Geology* 81.6, 683–692.

Dobeš, M., V. Bayer, and J. Polanský (1967). Kladensko-rakovnická pánev, přehodnocení geofyzikálních prací. Tech. rep. Geofyzika, Praha.

Dörr, W., J. Fiala, Z. Vejnar, and G. Zulauf (1998). structural development of metagranitoids of the Teplá crystalline complex: evidence for pervasive Cambrian plutonism within the Bohemian massif (Czech Republic). *Geologische Rundschau* 87, 135–149.

Dörr, W., G. Zulauf, J. Fiala, W. Franke, and Z. Vejnar (2002). Neoproterozoic to Early Cambrian history of an active plate margin in the Teplá–Barrandian unit | a correlation of U-Pb isotopic-dilution-TIMS ages (Bohemia, Czech Republic). *Tectonophysics* 352.1–2, 65–85.

Drost, K., U. Linnemann, N. McNaughton, O. Fatka, P. Kraft, M. Gehmlich, C. Tonk, and J. Marek (2004). New data on the Neoproterozoic Cambrian geotectonic setting of the Teplá-Barrandian volcano-sedimentary successions: geochemistry, U-Pb zircon ages, and provenance (Bohemian Massif, Czech Republic). *International Journal of Earth Sciences* 93.5, 742–757.

Dudek, A. (1980). The crystalline basement block of the outer Carpathians in Moravia – Brunovistulicum. Vol. 90. Rozpravy Československé Akademie věd, Řada matematika – přírodní vědy.

Faryad, S. W. (2012). High-pressure polymetamorphic garnet growth in eclogites from the Mariánské Lázně Complex (Bohemian Massif). *European Journal of Mineralogy* 24.3, 483–497.

Fiala, F. (1958). Hlavní typy hornin v širším okolí Pramenů v Císařském lese. Vol. 50. Geologické práce. Bratislava.

Finger, F., P. Hanžl, C. Pin, A. Von Quadt, and H. P. Steyer (2000). The Brunovistulian: Avalonian Precambrian sequence at the eastern end of the Central European Variscides? In: *Orogenic Processes, Quantification and Modelling in the Variscan Belt*. Ed. by W. Franke, V. Haak, O. Oncken, and D. Tanner. Vol. 179. Geological Society of London, Special Publications, 103–112.

Franke, W. (2000). The mid-European segment of the Variscides: tectonostratigraphic units, terrane boundaries and plate tectonic evolution. In: *Orogenic Processes, Quantification and Modelling in the Variscan Belt*. Ed. by W. Franke, V. Haak, O. Oncken, and D. Tanner. Vol. 179. Geological Society of London, Special Publications, 35–61.

Franke, W. (2006). The Variscan orogen in Central Europe: construction and collapse. *Geological Society, London, Memoirs* 32.1, 333–343.

Glodny, J., B. Grauert, J. Fiala, Z. Vejnar, and A. Krohe (1998). Metapegmatites in the western Bohemian massif: ages of crystallisation and metamorphic overprint, as constrained by U-Pb zircon, monazite, garnet, columbite and Rb-Sr muscovite data. *Geologische Rundschau* 87.1, 124–134.

Hajná, J., J. Žák, and V. Kachlík (2011). Structure and stratigraphy of the Teplá–Barrandian Neoproterozoic, Bohemian Massif: A new plate-tectonic reinterpretation. *Gondwana Research* 19.2, 495–508.

Hajná, J., J. Žák, V. Kachlík, and M. Chadima (2010). Subduction-driven shortening and differential exhumation in a Cadomian accretionary wedge: The Teplá–Barrandian unit, Bohemian Massif. *Precambrian Research* 176.1–4, 27–45.

Hickey, R. L., F. A. Frey, D. C. Gerlach, and L. Lopez-Escobar (1986). Multiple sources for basaltic arc rocks from the southern volcanic zone of the Andes (34–41° S): trace element and isotopic evidence for contributions from subducted oceanic crust, mantle, and continental crust. *Journal of geophysical Research* 91.B6, 5963–5983.

Hrouda, F., S. W. Faryad, M. Chlupáčová, and P. Jeřábek (2014). Magnetic fabric in amphibolized eclogites and serpentinized ultramafites in the Mariánské Lázně Complex (Bohemian Massif, Czech Republic): Product of exhumation-driven retrogression? *Tectonophysics* 629, 260–274.

Cháb, J. and V. Žáček (1994). Metamorphism of the Teplá Crystalline Complex. *KTB Report* 3, 33–37.

Jelínek, E., V. Štědrá, and J. Cháb (1997). The Mariánské Lázně Complex. In: *Geological model of western Bohemia related*

to the KTB borehole in Germany. Ed. by S. Vrána and V. Štědrá. Vol. 47. Prague: Czech Geological Survey, 32–36.

Kachlík, V. (1997). Contact-metamorphic rocks from the mantle of the Lestkov Pluton and their significance for reconstruction of the tectonometamorphic development of the Teplá-Barrandian Unit. Geoscience Research Reports for 1996. Czech Geological Survey, Prague.

Kalvoda, J., O. Bábek, O. Fatka, J. Leichmann, R. Melichar, S. Nehyba, and P. Spaček (2008). Brunovistulian terrane (Bohemian Massif, Central Europe) from late Proterozoic to late Paleozoic: a review. *International Journal of Earth Sciences* 97.3, 497–518.

Kastl, E. and J. Tonika (1984). The Mariánské Lázně metaophiolitic complex (West Bohemia). *Krystalinikum* 17, 59–76.

Konopásek, J. and K. Schulmann (2005). Contrasting Early Carboniferous field geotherms: evidence for accretion of a thickened orogenic root and subducted Saxothuringian crust (Central European Variscides). *Journal of the Geological Society* 162.3, 463–470.

Košler, J., D. R. Bowes, J. Konopásek, and J. Míková (2004). Laser ablation ICPMS dating of zircons in Erzgebirge orthogneisses evidence for Early Cambrian and Early Ordovician granitic plutonism in the western Bohemian Massif. *European Journal of Mineralogy* 16.1, 15–22.

Kotková, J., P. J. O'Brien, and M. A. Ziemann (2011). Diamond and coesite discovered in Saxony-type granulite: Solution to the Variscan garnet peridotite enigma. *Geology* 39.7, 667–670.

Kröner, A., A. P. Willner, E. Hegner, A. Frischbutter, J. Hofmann, and R. Bergner (1995). Latest precambrian (Cadomian) zircon ages, Nd isotopic systematics and P-T evolution of granitoid orthogneisses of the Erzgebirge, Saxony and Czech Republic. *Geologische Rundschau* 84.3, 437–456.

Kříbek, B., Z. Pouba, V. Skoček, and J. Waldhausrová (2000). Neoproterozoic of the Teplá-Barrandian Unit as a part of the Cadomian orogenic belt: a review and correlation aspects. *Bulletin of Geosciences* 75, 96–175.

Lexa, O., K. Schulmann, V. Janoušek, P. Štípská, A. Guy, and M. Racek (2011). Heat sources and trigger mechanisms of exhumation of HP granulites in Variscan orogenic root. *Journal of Metamorphic Geology* 29.1, 79–102.

Massonne, H. J. (2006). Early metamorphic evolution and exhumation of felsic high-pressure granulites from the north-western Bohemian Massif. *Mineralogy and Petrology* 86.3-4, 177–202.

Matte, P., H. Maluski, P. Rajlich, and W. Franke (1990). Terrane boundaries in the Bohemian Massif: result of large-scale Variscan shearing. *Tectonophysics* 177.1, 151–170.

Medaris, G. J., H. Wang, E. Jelínek, M. Mihaljevič, and P. Jakeš (2005). Characteristics and origins of diverse Variscan peridotites in the Gföhl Nappe, Bohemian Massif, Czech Republic. *Lithos* 82.1–2. Magmatic and Metamorphic Evolution of the Variscan Orogenic Crust Geology without Frontiers: Magmatic and Metamorphic Evolution of Central European Variscides, 1–23.

Medaris, L., E. Jelínek, S. W. Faryad, and B. S. Singer (2011). Peridotite and Metabasic Rocks of the Mariánské Lázně Metaophiolite Complex. *Geolines* 23, 71–83.

Mengel, K. and H. Kern (1992). Evolution of the petrological and seismic Moho – implications for the continental crust-mantle boundary. *Terra Nova* 4.1, 109–116.

O'Brien, P. J. and D. A. Carswell (1993). Tectonometamorphic evolution of the Bohemian Massif: evidence from high pressure metamorphic rocks. *Geologische Rundschau* 82.3, 531–555.

O'Brien, P. J. (1997). Garnet zoning and reaction textures in overprinted eclogites, Bohemian Massif, European variscides: a record of their thermal history during exhumation. *Lithos* 41.1-3, 119–133.

Patočka, F., P. Vlašímský, and K. Blechová (1993). Geochemistry of early Paleozoic volcanics of the Barrandian basin (Bohemian Massif, Czech Republic): Implications for paleotectonic reconstructions. *Jahrbuch der Geologischen Bundesanstalt* 136.4, 873–896.

Pin, C. and J. Waldhausrová (2007). Sm-Nd isotope and trace element study of Late Proterozoic metabasalts ("spilites") from the Central Barrandian domain (Bohemian Massif, Czech Republic). *Geological Society of America Special Papers* 423, 231–247.

Powell, R., T.J.B. Holland, and B. Worley (1998). Calculating phase diagrams involving solid solutions via non-linear equations, with examples using THERMOCALC. *Journal of Metamorphic Geology* 16, 577–588.

Růžek, B., V. Vavryčuk, P. Hrubcová, and J. Zedník (2003). Crustal anisotropy in the Bohemian Massif, Czech Republic: Observations based on Central European lithospheric experiment based on refraction (CELEBRATION) 2000. *Journal of Geophysical Research: Solid Earth* 108.B8, 2392, doi:10.1029/2002JB002242.

Seifert, A., ed. (2012). Vysvětlivky k základní geologické mapě ČR list Jesenice 12133. Česká geologická služba.

Schulmann, K., O. Lexa, V. Janoušek, J. M. Lardeaux, and J. B. Edel (2014). Anatomy of a diffuse cryptic suture zone: An example from the Bohemian Massif, European Variscides. en. *Geology* 42.4, 275–278.

Schulmann, K., J. Konopásek, V. Janoušek, O. Lexa, J.-M. Lardeaux, J.-B. Edel, P. Štípská, and S. Ulrich (2009). An Andean type Palaeozoic convergence in the Bohemian Massif. *Comptes Rendus Geoscience* 341.2-3, 266–286.

Siebel, W., H. Raschka, W. Irber, H. Kreuzer, K. L. Lenz, A. Höhndorf, and I. Wendt (1997). Early Palaeozoic acid magmatism in the Saxothuringian Belt: new insights from a geochemical and isotopic study of orthogneisses and metavolcanic rocks from the Fichtelgebirge, SE Germany. *Journal of Petrology* 38.2, 203–230.

Stosch, H. G. and G. W. Lugmair (1990). Geochemistry and

evolution of MORB-type eclogites from the Münchberg Massif, southern Germany. *Earth and Planetary Science Letters* 99.3, 230–249.

Strnad, L. and M. Mihaljevič (2005). Sedimentary provenance of Mid-Devonian clastic sediments in the Teplá-Barrandian Unit (Bohemian Massif): U–Pb and Pb–Pb geochronology of detrital zircons by. *Mineralogy and Petrology* 84.1-2, 47–68.

Suess, F. E. (1926). Intrusionstektonik und Wandertektonik im variszischen Grundgebirge. Gebrüder Borntraeger, Berlin.

Štědrá, V. (1994). Amphibolite facies metamorphism of the Mariánské Lázně complex. *Journal of Czech Geological Society, Conference abstracts* 39.1, 111.

Štědrá, V. (2001). Tectonometamorphic evolution of the Mariánské Lázně Complex, Western Bohemia, based on the study of metabasic rocks. PhD thesis. Charles University, Prague.

Štědrá, V., V. Kachlík, and R. Kryza (2002). Coronitic metagabbros of the Mariánské Lázně Complex and Teplá Crystalline Unit: inferences for the tectonometamorphic evolution of the western margin of the Teplá-Barrandian Unit , Bohemian Massif. In: *Palaeozoic amalgamation of Central Europe: an introduction and synthesis of new results from recent geological and geophysical investigations*. Ed. by J. A. Winchester, T. C. Pharaoh, and J. Verniers. 201. Geological Society of London, Special Publications, 217–236.

Tait, J. A., V. Bachtadse, W. Franke, and H. C. Soffel (1997). Geodynamic evolution of the European Variscan fold belt: palaeomagnetic and geological constraints. *Geologische Rundschau* 86.3, 585–598.

Tichomirowa, M., H. J. Berger, E. A. Koch, B. V. Belyatski, J. Götze, U. Kempe, L. Nasdala, and U. Schaltegger (2001). Zircon ages of high-grade gneisses in the Eastern Erzgebirge (Central European Variscides)|constraints on origin of the rocks and Precambrian to Ordovician magmatic events in the Variscan foldbelt. *Lithos* 56.4, 303–332.

Timmermann, H., W. Dörr, E. Krenn, F. Finger, and G. Zulauf (2006). Conventional and in situ geochronology of the Teplá Crystalline unit, Bohemian Massif: implications for the processes involving monazite formation. *International Journal of Earth Sciences* 95.4, 629–647.

Timmermann, H., V. Štědrá, A. Gerdes, S. Noble, R. Parrish, and W. Dörr (2004). The problem of dating high-pressure metamorphism: a U-Pb isotope and geochemical study on eclogites and related rocks of the Mariánske Lázně Complex, Czech Republic. *Journal of Petrology* 45.7, 1311–1338.

Tollmann, A. (1982). Großräumiger variszischer Deckenbau im Moldanubikum und neue Gedanken zum Variszikum Europas. Vol. 64. Geotektonische Forschungen. Schweizerbart Science publishers.

Tomek, C., V. Dvořáková, and S. Vrána (1997). Geological interpretation of the 9HR and 503M seismic profiles in western Bohemia. In: *Geological model of western Bohemia related to the KTB borehole in Germany*. Ed. by S. Vrána and V. Štědrá. Vol. 47. Prague: Czech Geological Survey, 43–51.

Vejnar, Z. (1984). Geologie domažlické oblasti. Ústřední ústav geologický, Praha.

Venera, Z., K. Schulmann, and A. Kröner (2000). Intrusion within a transtensional tectonic domain: the Čistá granodiorite (Bohemian Massif)|structure and rheological modelling. *Journal of Structural Geology* 22, 1437–1454.

Zulauf, G. (1997a). Constriction due to subduction: evidence for slab pull in the Mariánské Lázně complex (central European Variscides). *Terra Nova* 9, 232–236.

Zulauf, G. (1997b). From very low-grade to eclogite-facies metamorphism: tilted crustal sections as a consequence of Cadomian and Variscan orogeny in the Teplá–Barrandian unit (Bohemian Massif). Vol. 89. Geotektonische Forschungen. E. Schweizerbartsche Verlagsbuchhandlung, 1–302.

Zulauf, G. (2001). Structural style, deformation mechanisms and paleodifferential stress along an exposed crustal section: constraints on the rheology of quartzofeldspathic rocks at supra- and infrastructural levels (Bohemian Massif). *Tectonophysics* 332.1-2, 211–237.

Zulauf, G., W. Dörr, J. Fiala, and Z. Vejnar (1997). Late Cadomian crustal tilting and Cambrian transtension in the Teplá–Barrandian unit (Bohemian Massif, Central European Variscides). *Geologische Rundschau* 86.3, 571–584.

Žáček, V. and J. Cháb (1993). Metamorphism in the Tepla upland, Bohemian massif, Czech Republic (preliminary report). *Věstník Českého geologického ústavu* 68.3, 33–37.

Žáček, V. and J. Cháb (1998). Výsledky doplňkového výzkumu metamorfózy a tektoniky tepelského krystalinika. Tech. rep. Český geologický ústav, Praha.

Žáček, V. (1999). Kyanite Pseudomorphs after Andalusite from the Teplá Crystalline Complex-Evidence for Pre-Variscan Low-Pressure Metamorphism. *Geolines* 8, 1998–1999.

14 millions years of the volcanic history of Doupovské hory Volcanic Complex

Vladislav Rapprich and Michael Petronis

The Bohemian Massif experienced intense magmatic and volcanic activity during the Cenozoic. The intracontinental within-plate alkaline magmatism was associated with the formation of the Eger Rift (ER), which forms the NE branch of the European Cenozoic Rift System (ECRIS; Dèzes et al., 2004). The ER strikes across the western part of the Bohemian Massif in the ENE–WSW direction, roughly following the Variscan suture zone between the Saxothuringian and Teplá–Barrandian domains of the Bohemian Massif (Mlčoch and Konopásek, 2010).The incipient rift system of the ER underwent two distinct phases of extension (Rajchl et al., 2009). NNE–SSW to N–S oriented horizontal extension during the first phase of rifting which occurred between the end of Eocene and early Miocene. The trend of the extension was oblique to the rift axis and caused the evolution of a fault system characterised by en-echelon arranged

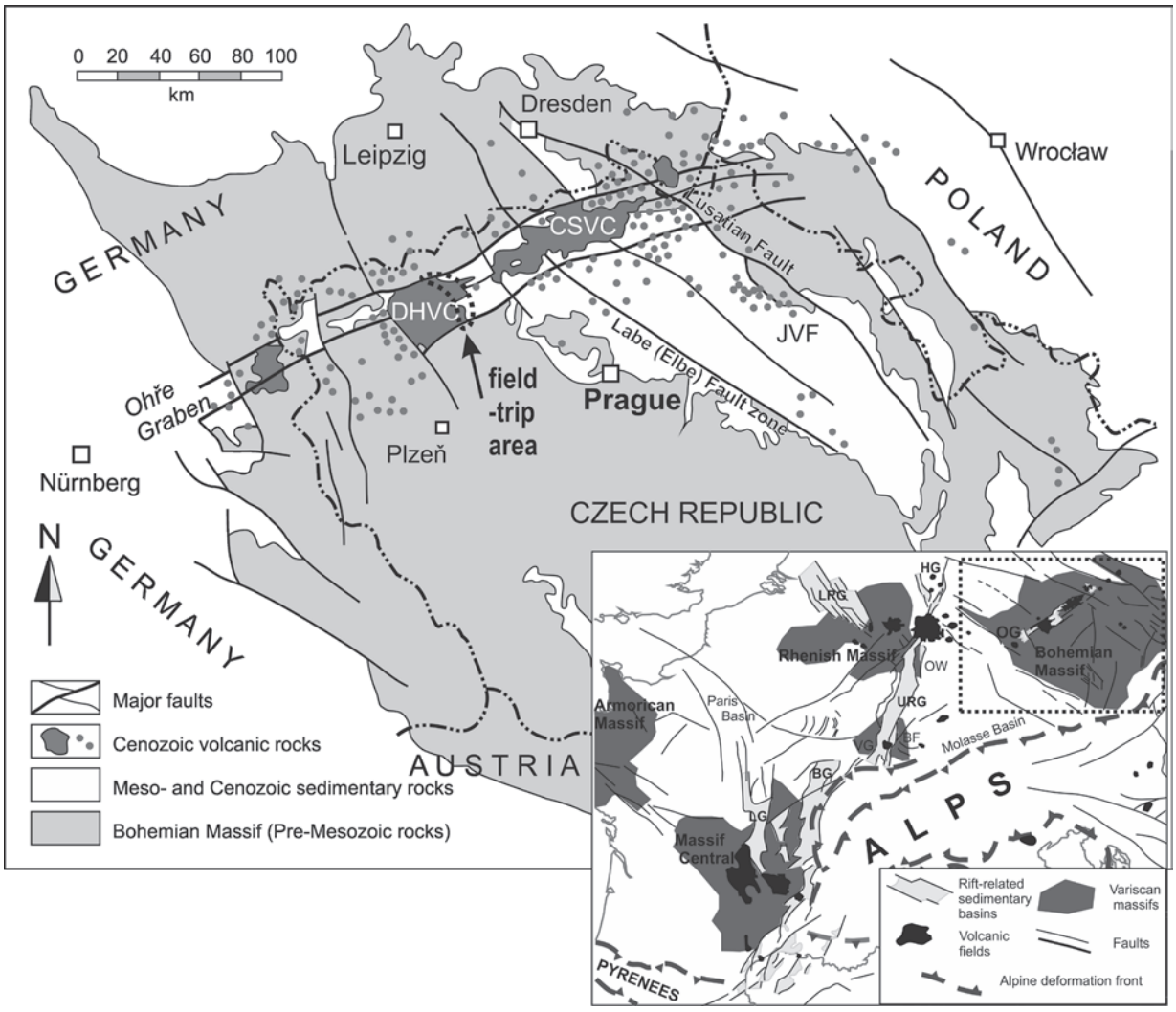

Fig. 1: Distribution of Cenozoic alkaline volcanic rocks in the Bohemian Massif. DHVC – Doupovské hory Volcanic Complex, CSVC – České středohoří Volcanic Complex. Position of Bohemian Massif within the European Variscides and Eger Graben as a part of the ECRIS shown in inset.

E–W (ENE–WSW) faults. A number of small, shallow initial depo-centres formed in this fault system (Rajchl et al., 2009). The origin of the palaeostress field of the oblique, extensional phase seems to be most likely a result of doming due to thermal perturbation of the lithosphere (Dèzes et al., 2004). The later phase had an extension direction orthogonal to the rift axis. This is explained by stretching along the crest of a growing regional- scale anticlinal feature, which supports the recent hypothesis of lithospheric folding in the Alpine-Carpathian foreland (Dèzes et al., 2004; Bourgeois et al., 2007; Rajchl et al., 2009).

The Eger Rift contains two large volcanic complexes including subvolcanic intrusions – the České středohoří Volcanic Complex (CSVC) in the NE part and the Doupovské hory Volcanic Complex (DHVC) in the SW part (Fig. 1).

Our field-trip is focused on Doupovské hory – volcanic complex which preserves a 14 million year history of volcanism including periods of volcanic edifice growth and periods of edifice failure. The Oligocene–Lower Miocene Doupovské hory Volcanic Complex (DHVC) is little affected by erosion with still well-preserved original volcanic morphology. Formation of the DHVC started during the Lowermost Oligocene (Fejfar and Kaiser, 2005) by predominantly explosive activity. Soon after, the activity shifted towards effusions of mostly basaltic lavas (Rapprich and Holub, 2008). The lava sequences reach thickness of several hundred meters. A body of subvolcanic rocks intruded into the early DHVC edifice in Lower Oligocene (Holub et al., 2010). The latest lavas were erupted in Lower Miocene (ca 20 Ma: Ulrych et al., 2003; Sakala et al., 2010). The growth of the volcano was several times interrupted by periods of volcano decay and collapses producing debris flows and debris avalanches (e.g. Sakala et al., 2010). Two distinct suites of volcanic and intrusive rocks were identified within the DHVC. Both suits comprise primitive mafic members (basanites, olivine nephelinites, alkali basalts, tephrites, ijolites, essexites) as well as rocks at different stage of differentiation (trachybasalts, trachyandesites, trachytes, phonolites, foid-monzonites, foid-syenites, urtites). Both series were contemporaneously active throughout the entire history of the DHVC (Rapprich and Holub, 2008; Holub et al., 2010). The tephrite/alkalibasalt – trachybasalt – trachyandesite – trachyte (essexite – foid-syenite) suite has mineral assemblage containing hydrous minerals and more radiogenic Sr-Nd isotopic signature. The olivine nephelinite – basanite – tephriphonolite – phonolite (melteigite – ijolite – urtite) suite contains primitive members rich in olivine, is free of hydrous minerals and displays more depleted Sr-Nd isotopic signature (Rapprich and Holub, 2008; Holub et al. 2010). During the field trip, characteristic localities for different stages and processes of the DHVC evolution will be visited on the eastern margins of the DHVC (Fig. 2), which is in its dominant part occupied by military training area and therefore not accessible.

Fig. 2: Map of the field trip route:

1 – Dětaň, abandoned quarry in Early Oligocene pyroclastic deposits;

2 – Radechov, natural outcrop in sequence of Late Oligocene – Early Miocene lahar deposits;

3 – Úhošť Hill, outcrops in sequence of Oligocene – Early Miocene alkali basalt lavas;

4 – Klášterec upon Ohře, outcrops in deposits of Early Oligocene debris avalanches;

5 – Šumná, remnant of Early Miocene scoria cone with trachybasaltic lava flow.

Stop 1 – Dětaň, abandoned quarry

GPS coordinates: 50.1886031N, 13.3024033E
Focus of the stop: Early Oligocene pyroclastic deposits

The earliest volcanic deposits of the DHVC are exposed on its SE margins, around Dětaň, Dvérce and Valeč. These earliest volcanic rocks are represented by up to 80 m thick sequence of layered pyroclastic deposits (Fig. 3). The tuffs, lapilli-tuffs and lapilli-stones are exposed in an abandoned quarry, which was exploiting kaolin underneath the pyroclastic rocks. The exposures of pyroclastic deposits around Dětaň, Valeč and Dvérce are important and intensively studied paleontological localities (e.g., Fejfar and Kaiser, 2005). The assemblage of mammal bones and teeth (rodents, hyenodonts, entelodonts, rhinos, etc.) found in these sequences correspond to mammal zone MP21 giving the exact age of the initial phase of DHVC activity to the very early Oligocene.

In the Dětaň quarry, we can see sequences of tuff and lapilli layers differing slightly in colour and grain-size. The lowermost layer with signs of diagonal cross bedding, which is also the main fossiliferous bed, and most likely represents pyroclastic surge deposits from a maar eruption. Good sorting and massive texture of the overlying layers suggest fall deposition. These pyroclastic deposits exposed at Dětaň were formerly interpreted as products of explosive eruptions from a central volcano in the middle of the DHVC, some 16 km to the NW from Dětaň. However, in the other parts of the DHVC, comparable pyroclastic sequence are not found in other parts of the DHVC. Following the Dětaň pyroclastic sequence in outcrops available in near surroundings, rapid change in individual bed thickness as well as in the grain-size (up to coarse scoria beds) can be observed over a few meters distance. Such dramatic changes are inconsistent with the posed origin of these deposits as distal deposits of large eruptions from a single central volcano. The observed distribution of pyroclastic rocks are more likely related to the field of small monogenetic volcanoes located in different directions from Dětaň. Additional data on early DHVC volcanic activity were obtained from N-1 drilling some 3 km SW from Dětaň. This drilling penetrated pyroclastic deposits identical to the Dětaň sequence. Clast-supported well-sorted deposits exposed in this drilling were dominated by angular clasts of non-vesicular basaltoid suggesting phreatomagmatic eruption. The bedding of these deposits are dipping some 30° suggesting slope facies of a phreatomagmatic tuff-cone were recorded by this drilling underneath younger lahar deposits. In summary, the pyroclastic sequence at Dětaň represents a group of monogenetic volcanoes including scorian cones, tuff cones and maars supplying the studied locality with pyroclastic fall deposits of variable grain-size and structure.

Fig. 3: Layered pyroclastic deposits exposed in the abandoned quarry in Dětaň.

Fig. 4: Ill-sorted clast-supported pyroclastic deposits in the N-1 drill-core (from Rapprich, 2011).

Stop 2 – Radechov, natural outcrop

GPS coordinates: 50.2775172N, 13.2643503E
Focus of the stop: Sequence of Late Oligocene – Early Miocene lahar deposits

The second stop will lead us to an amazing outcrop in more than 200 m thick sequence of lahar deposits interbedded with several lava flows. The outcrops known as V Jámách near Radechov are not accessible by bus that must be left in Vojtěchov. From Vojtěchov, the site of interest requires a 2 km walk. The landscape in this area is characterized by E-W elongated ridges resembling hummocky relief. As we walk over the lahar fan on the volcano foothills, recognize that this relief does not reflect the original hummocks of debris avalanches. Rather the elongated ridges are the result of erosion of a thick lahar deposit, where erosion follows individual channels and tongues of the lahars. An interesting view of the morphology of the DHVC will be seen approximately after 1 km of walking. Gently dipping slopes of the volcanic edifice can be seen well from this view-point. These slopes reflect surfaces of basaltic lava flows of a low viscosity. Morphology is one of the arguments against the hypothesis that the DHVC represent an erosional remnant of a single stratovolcano. The gentle slopes of a volcano dominated by basaltic lavas correspond to a shield volcano and the observed morphology can be well compared with Hawaiian volcanoes like Mauna Loa or Maune Kea.

Once we reach the outcrop, a total of 50 m high rock-walls expose deposits of the lahars interbedded with lava flows. According to available borehole data, this outcrop exposes only one fourth of the entire sequence. The sequence consists of numerous flow units with variable texture (Fig. 5). Each flow unit reaches 1–1.5 m in thickness. Some units are clast-supported while the others are matrix-supported reflecting water-saturation in the mass-flow. Occasionally, up to 2 m large boulders can be found floating in the lahar deposit which had high cohesion (Fig. 6). Most of the flow units have preserved fine-grained layer atop, representing reworking of fine material during the latest stage of lahar deposition. These fine-grained layers highlight morphological boundaries between individual layers.

The lahars are also interbedded with three lava flows. The composition of these lavas shows a differentiation trend from olivine bearing trachybasal, basaltic trachyandesite to trachyandesite. Such compositions are not common in the DHVC, and the source vent of these lavas can be therefore traced to the hill Nad Hájenou (495 m), 1 km to the SW from the locality. The final stage of the differentiation is represented by a phonolite, which was not able to expand out of Nad Hájenkou Hill due to its high viscosity. The trachybasaltic to trachyandesitic lava flows are coated with a carapace facies of autoclastic breccia. The autoclastic breccias are clast-supported with empty voids and consist of angular fragments of the lava. The autoclastic breccias are formed due to mechanical fragmentation of solidified crust of continuously moving lava (Fig. 7). Geochronological analyses of the lavas (25.5, 24.6 and 26.9 Ma, Fig. 5) constrain the age of this lahar sequence. The main triggering process producing this lahar succession was the instability of the south-eastern sector of the DHVC due to heterogeneous basement. Most of the DHVC basement consists of Variscan metamorphic and plutonic rocks (granites, amphibolites, gneisses, phylites, etc.), but tectonically limited Žatec Basin with up to 800 m of Permo-Carboniferous sedimentary infill plunges underneath the DHVC to the SE (Mlčoch and Konopásek, 2010). The heterogeneous plastic sediments were not able to carry the load of the thick sequence of basaltic lavas with high specific weight. This resulted in sector spreading of the volcanic complex producing frequent debris flows (Fig. 8).

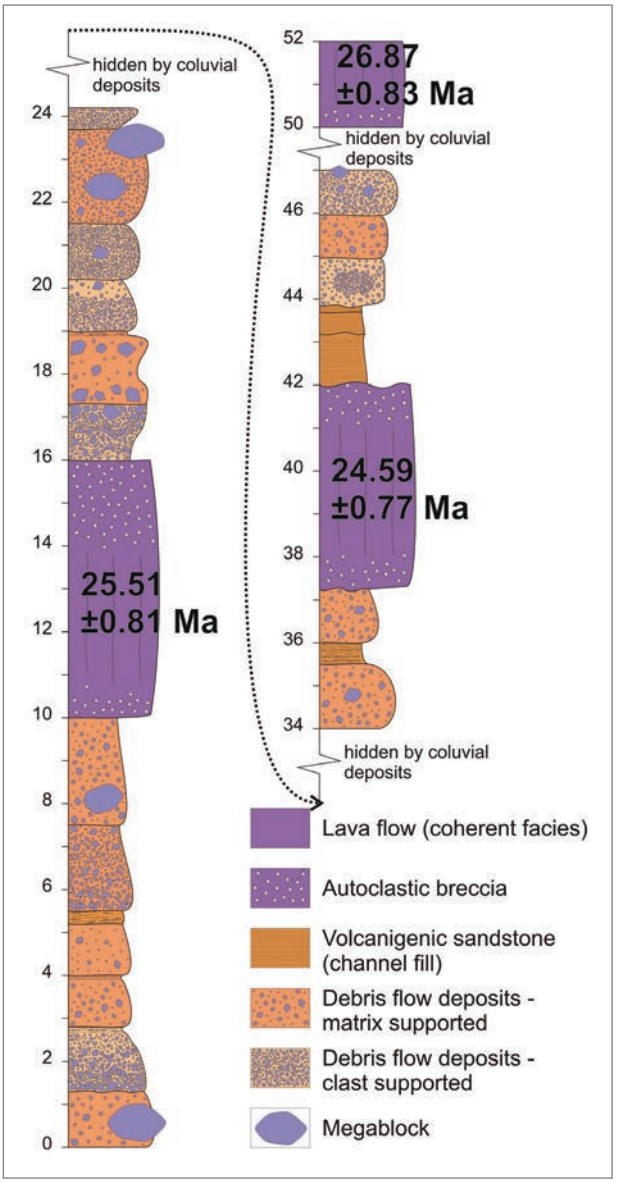

< Fig. 5: Scheme of the lahar units exposed on the cliff at Radechov.

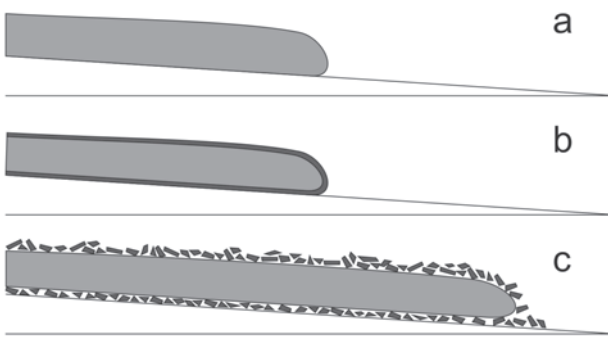

Fig. 7: Mechanism of autoclastic breccia generation.

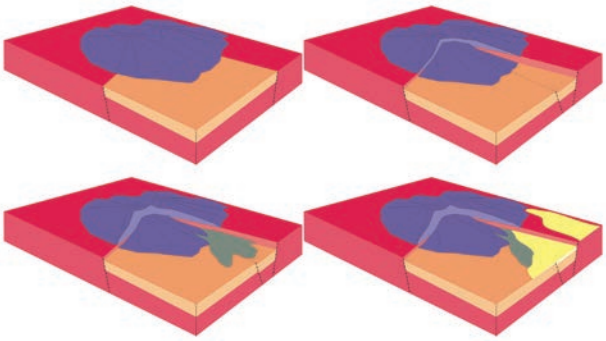

Fig. 8: Schematic evolution of the failure of the south-eastern segment of the DHVC.

Fig. 6: Large boulder (2 m) in lahar deposit at Radechov.

Stop 3 – Úhošť Hill

GPS coordinates: 50.3602561N, 13.2541353E
Focus of the stop: Sequence of Oligocene – Early Miocene alkali basalt lavas

At the previous locality, we observed the morphology of the DHVC resembling the Hawaiian shield volcano. At the third site, we will observe dominant lithologies of this volcanic area. Already in the Early Oligocene, after the formation of the field of monogenetic volcanoes near Dětaň, the volcanic activity of the DHVC was dominated by effusions of numerous basaltic lavas lasting until Early Miocene. This continuous effusive activity was several times interrupted by volcanic edifice failure, but new lavas soon filled the open space again. Úhošť Hill is a typical example of accumulation of basaltic lavas in the DHVC. Nine lava flows were identified during detailed research (Fig. 9), with thickness usually not exceeding 5 m (except for the thick youngest lava). Most of the lavas are coated with autoclastic breccia, which was formerly erroneously interpreted as a pyroclastic deposits and the Úhošť profile as an example of stratovolcanic structure applied to the entire DHVC. As shown in Radechov, autoclastic breccia is clast supported and monomictic consisting solely of fragments of related lavas. The interclast voids remain empty or can be later filled with younger sedimentary or pyroclastic material.

The observed geochemical evolution in the sequence of Úhošť lavas cannot be explained in terms of simple magma evolution or exhausting of stratified magma chamber. The observed rocks belong to two alternating independent suites. One suite comprise nephelinite, tephrite, basanite and picrobasalt (flows 1, 2, 3, 5 and 6). The picrobasalts represent semicumulitic rocks enriched in clinopyroxene and olivine phenocrysts derived from basanites. This suite therefore represents continuous exhausting of a zoned magma chamber with melts depleted in phenocrysts (nephelinite and tephrite) erupted first and the magma enriched in phenocrysts erupted as the last. This suite has uniform isotopic composition ($^{87}Sr/^{86}Sr_i$ 0.70409–0.70418, $^{143}Nd/^{144}Nd_i$ 0.51270–0.51271). The second suite consisting of alkali basalts that contain pseudomorphs after amphibole, not present in the tephrite-basanite-picrobasalt suite. The basalts of the alkali basalt suite are higher in silica and aluminium and also their isotopic signature differs significantly ($^{87}Sr/^{86}Sr_i$ 0.70452–0.70459, $^{143}Nd/^{144}Nd_i$ 0.512661–0.512665; Rapprich and Holub, 2008). These data are interpreted to reflect that the erupted magmas were fed from distinct sources. Synchronous alternating activity of magmas from different source was also documented in the intrusive system in the central part of the DHVC (Holub et al., 2010). The K-Ar geochronology dates the activity of the Úhošť lavas to a time-span from 28 Ma–22 Ma (Rapprich and Holub, 2008).

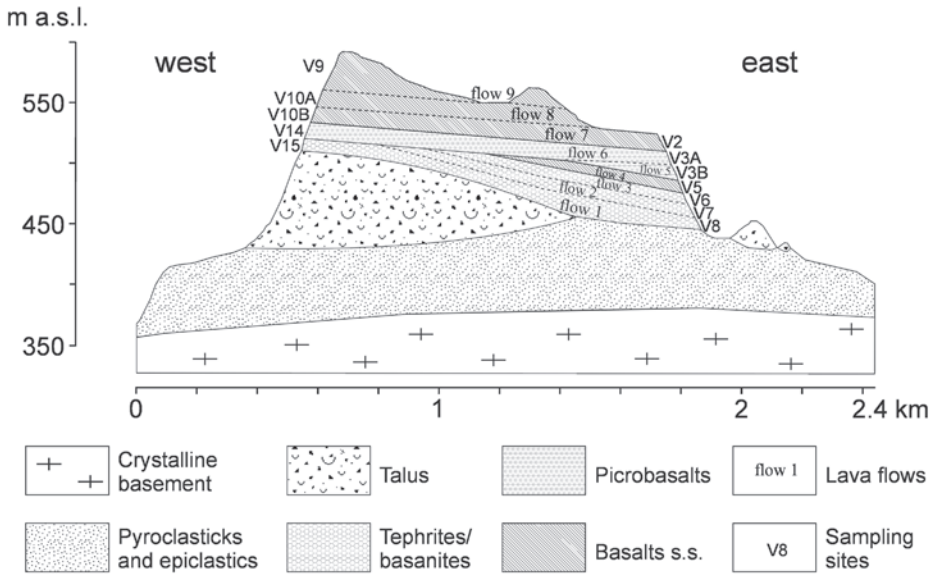

Fig. 9. Cross section of Úhošť Hill with individual lava flows identified (from Rapprich and Holub, 2008).

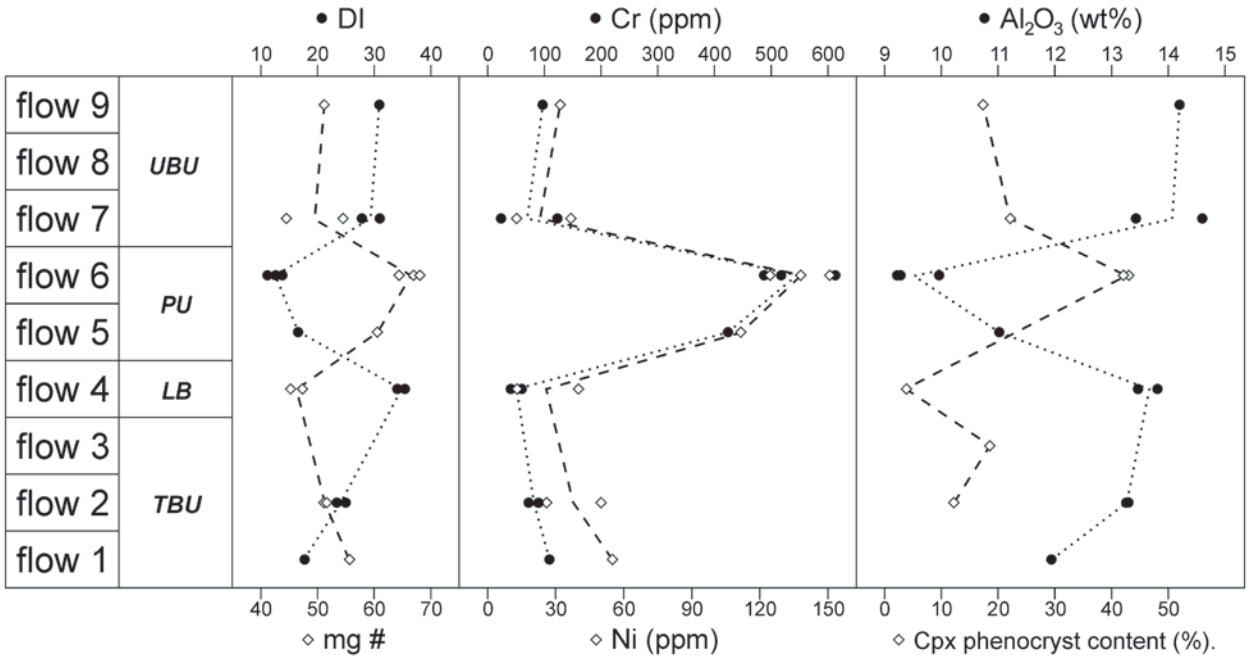

Fig. 10: Compositional evolution of Úhošť lavas (from Rapprich and Holub, 2008). DI – differentiation index (sum of felsic minerals except of anortite calculated from CIPW-norm), TBU – tephrite/basanite unit, LB – lower basalt, PU – picrobasalt unit, UBU – upper basalt unit.

Stop 4 – Klášterec nad Ohří, outcrops

GPS coordinates: 50.3921644N, 13.1857678E
Focus of the stop: Deposits of Early Oligocene debris avalanches

At the second stop, we have visited deposits of debris- and hyperconcentrated flows (lahars), but the DHVC experience provides much more dramatic examples of the processes associated with the failure of volcanic edifice. The eastern foothill of the DHVC is not the only lahar fan present in the peripheries of the DHVC. Another important and extensive fan of debris flow deposits can be found on the northern slopes, where Kadaň and Klášterec Towns were built. These deposits are generally older than those visited near Radechov (capped by a 28 Ma lavas) and also more affected by erosion. One important feature, however, can be seen in several places around Klášterec. Large blocks (up to several meters) are fragmented to subgrains, but the sub-grains remain in jig-saw fit structure and do not migrate away from each other (Fig. 11). Such a structure is characteristic for debris avalanches, those are able to carry mega-blocks and move as plug-flows. Such deposits provide evidence that large segments of the Early DHVC volcano edifice underwent edifice collapses. The collapse producing avalanches exposed around Klášterec occurred most likely in the area of Lesná Hill (812 m), and the empty space was filled and buried by lavas of the ongoing volcanic activity.

Fig. 11: Jig-saw fit of subgrains in a megablock within the debris avalanche deposit in the DHVC.

Stop 5 – Šumná Hill

GPS coordinates: 50.3728761N, 13.1467031E
Focus of the stop: Remnant of Early Miocene scoria cone with trachybasaltic lava

The volcanic activity of the DHVC ceased out about 20 Ma. The latest activity is represented by a group of scoria cones in the northern part of the DHVC (Sakala et al., 2010) and some lava flows in south (Ulrych et al., 2003). The last locality of our field trip represents the very youngest eruption within the DHVC. Šumná Hill penetrates Oligocene debris flows and debris avalanches deposits and rises above the Klášterec – Karlovy Vary road. The strategic position of this hill situated between an important historical road and the Ohře River was the main reason for construction of a medieval castle. In the trenches of the castle, pyroclastic deposits of this small volcano are well exposed. The deposits consist of coarse, clast-supported scoriae with empty voids between clasts. Two layers of scoria are separated by reddish fine ash, probably representing fall deposit from some distant source. These deposits correspond to near-vent facies of a scoria cone erupting in Strombolian style eruptions. The scoria cone erupted lava flows covering the plain north of the volcano. The K-Ar analyses determined the age of this volcano as 20 Ma (Sakala et al., 2010).

Fig. 12: Šumná Hill rising above the Klášterec Karlovy Vary road.

Fig. 13: Scoria deposits on the Šumná scoria cone.

References

Bourgeois, O., Ford, M., Diraison, M., Le Carlier De Veslud, C., Gerbault, M., Pik, R., Ruby, N., Bonnet, S. (2007): Separation of rifting and lithospheric folding signatures in the NW-Alpine foreland. – International Journal of Earth Sciences (Geologishe Rundschau), 96: 1003–1031.

Dèzes, P., Schmid, S.M., Ziegler, P.A. (2004): Evolution of the European Cenozoic Rift System: interaction of the Alpine and Pyrenean orogens with their foreland lithosphere. – Tectonophysics, 389: 1–33.

Fejfar, O., Kaiser, T.M. (2005): Insect bone-modification and paleoecology of Oligocene Mammal-bearing sites in the Doupov Mountains, Northwestern Bohemia. – Palaeontologia Electronica, 8A, 11p, http://palaeo-electronica.org/paleo/2005_1/fejfar8/issue1_05.htm

Holub, F. V., Rapprich, V., Erban, V., Pécskay, Z., Mlčoch, B., Míkova, J. (2010): Petrology and geochemistry of the Tertiary alkaline intrusive rocks at Doupov, Doupovské hory Volcanic Complex (NW Bohemian Massif). – Journal of GEOsciences, 55: 251–278.

Mlčoch, B., Konopásek, J. (2010): Pre-Late Carboniferous geology along the contact of the Saxothuringian and Teplá-Barrandian zones in the area covered by younger sediments and volcanics (western Bohemian Massif, Czech Republic). – Journal of Geosciences, 55: 81–94.

Rajchl, M., Uličný, D., Grygar, R., Mach, K. (2009): Evolution of basin architecture in an incipient continental rift: the Cenozoic Most Basin, Eger Graben (Central Europe). – Basin Research, 21: 269–294.

Rapprich, V. (2011): Vrt N-1 Valeč: sonda do počátku vývoje doupovského vulkanického komplexu / N-1 Valeč borehole: a searcher into the initial phase of the Doupovské hory Volcanic Complex. – Geoscience Research Reports for the year 2010: 41–45.

Rapprich, V., Holub, F.V. (2008): Geochemical variations within the Upper Oligocene–Lower Miocene lava succession of Úhošť Hill (NE margin of Doupovské hory Mts., Czech Republic). – Geological Quarterly, 52: 253–268.

Sakala, J., Rapprich, V., Pécskay, Z. (2010): Fossil angiosperm wood and its host deposits from the periphery of a dominantly effusive ancient volcano (Doupovské hory Volcanic Complex, Oligocene-Lower Miocene, Czech Republic): systematics, volcanology, geochronology and taphonomy. – Bulletin of Geosciences, 85: 617–629.

Ulrych, J., Lloyd, F.E., Balogh, K. (2003): Age relations and geochemical constraints of Cenozoic alkaline volcanic series in W Bohemia: a review. – Geolines, 15: 168–180.